

Hemilability and nonrigidity in metal complexes of bidentate $P,P=S$ donor ligands [☆]

J.W. Faller ^{*}, Suzanna C. Milheiro, Jonathan Parr

Yale University, P.O. Box 208107, New Haven, CT 06520-8107, United States

Received 28 August 2007; received in revised form 25 October 2007; accepted 25 October 2007

Available online 1 November 2007

Dedicated to the memory of F.A. Cotton.

Abstract

Hemilability and nonrigidity in a series of mixed $P,P=S$ donor ligands has been studied in the complexes $[\text{Pd}(P,P=S)\text{Cl}_2]$, $[\text{Pd}(\eta^3\text{-C}_3\text{H}_5)(P,P=S)[\text{SbF}_6]]$, and $[\text{Rh}(\text{cod})(P,P=S)[\text{SbF}_6]]$ ($P,P=S = \text{Ph}_2\text{P-Q-P(S)Ph}_2$). The effect of bite angle, the rigidity of the ligand backbone, and the role of the ancillary ligands are discussed.

© 2007 Elsevier B.V. All rights reserved.

Keywords: Hemilabile; Fluxional; Nonrigid

1. Introduction

Hemilabile ligands have played a key role in a number of important reactions catalyzed by transition-metal complexes [2–5]. As an example, a ligand combining a hard and soft donor atom, such as P,O can exist in $\kappa^2 \rightleftharpoons \kappa^1$ equilibria as shown in Scheme 1, in which the relative concentrations of O-bound and P-bound complexes depend upon the strengths of the M–P and M–O bonds.

In most cases the nature of the metal will allow one of the donors to dissociate; whereas the other metal–donor bond will be inert and the donor will be effectively anchored to the metal. The opening of the chelate can occur by a dissociative process or be initiated by solvent or other ligands. One of the early notable successes associ-

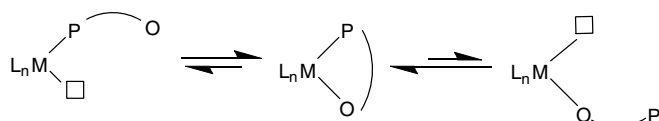
ated with P,O-ligands was their application in the Shell higher olefin process which utilizes a nickel-catalyzed oligomerization of ethylene [6]. More recent interest in hemilabile ligands for polymers has involved their use in copolymerizations of ethylene and carbon monoxide, and ethylene and acrylates [7–10].

The nature of the donor atoms of ligands have a significant influence on transition metal catalyzed reactions and the use of ligands containing more than one kind of donor has proven successful for some asymmetric reactions [11–13] including allylic substitution [14–16]. Heterobidentate ligands containing two different donors, often one hard and one soft donor, offer several advantages over traditional symmetrical bisphosphine ligands by creating steric and electronic asymmetry at the metal center [17]. A potential consequence of having donors with different properties is that hemilability [3] may become important in the reactions. During a catalytic cycle, dissociation of the more labile donor can create an open site for substrate binding, while re-coordination of that donor can temporarily stabilize a potentially coordinatively unsaturated metal center at another step in the catalytic process. Hemilability may have further applications in asymmetric catalysis

[☆] It was a pleasure to have collaborated with Al on seven of the original papers in the “Stereochemically Nonrigid Organometallic Molecules” series. F.A. Cotton’s reminiscences of our early work in this area from the 100th issue of JOMC provide an insight into his contributions in this area of using dynamic NMR to study mechanisms [1].

^{*} Corresponding author. Fax: +1 203 432 6144.

E-mail address: jack.faller@yale.edu (J.W. Faller).



Scheme 1. Hemilability.

where hemilabile ligands may allow interconversion of diastereomeric isomers to form a preferred isomer that could then serve as an asymmetric catalyst.

Although there are known examples of complexes of hemilabile ligands that are efficient catalysts [3], it is difficult to predict which ligands will have the proper combination of donor properties to be effective for a given reaction. If hemilability is required to provide an open coordination site, then (1) the strength of the metal–donor bond is important so that a sufficient fraction of open sites are available and (2) the rate of providing those sites must match the other kinetic parameters to allow the catalytic cycle to turn over at an acceptable rate. It is a challenge to observe hemilability in many systems because the spectroscopic response of the metal complex is often apparently unchanged during the dissociation and association of the labile functionality. In particular, if there is only a small fraction of the hemi-dissociated complex present, in many cases neither chemical shifts, nor couplings are modified sufficiently to provide detection of the hemilability by NMR. Further, if a fluxional process resulting from hemilability results in the interconversion of isomers that are distinguishable by techniques such as NMR, the relative stabilities of the isomers may influence the fluxional processes making it difficult to distinguish hemilability from other processes.

We have investigated several systems that allow the examination of hemilability using NMR spectroscopy. Using variable temperature ^1H , ^{13}C , and ^{31}P NMR, we have determined the barrier to hemilability for a series of palladium and rhodium complexes by observing the

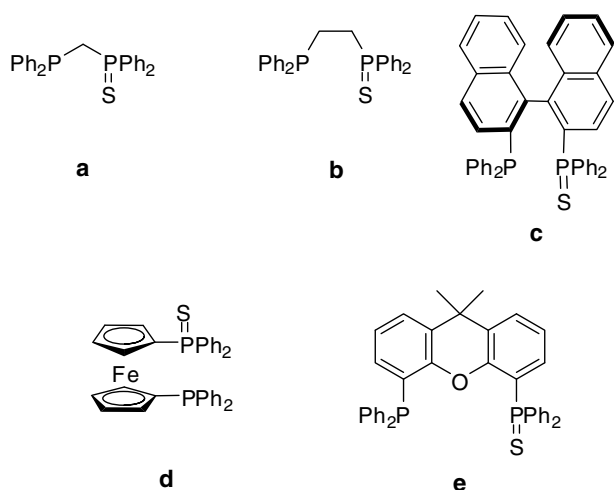
exchange of resonances from both the hemilabile ligand and from other ligands present on the metal. The effects of chelate ring size, of the rigidity of the ligand backbone on hemilability, and of η^3 -allyl fluxional processes are discussed within the context of the $P,P=S$ ligands shown in Fig. 1.

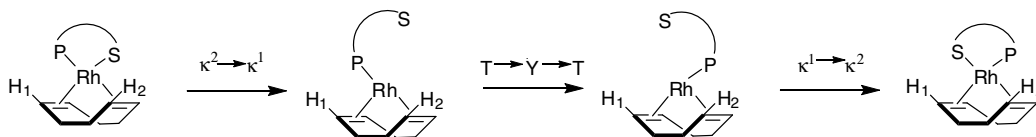
2. Results and discussion

2.1. $[\text{Rh}(\text{cod})(P,P=S)][\text{SbF}_6]$ complexes (**1**)

Although we ultimately wish to address hemilability in palladium allyl complexes, the potential for rearrangement of allyls via η^3 – η^1 – η^3 can complicate the issue. In order to limit the number of possible rearrangement processes, we prepared a series of rhodium diene complexes (diene = cod) that should be free of the multiple rearrangement pathways available to allyls. Utilizing some of the $P,P=S$ donor ligands in Fig. 1, hemilability could be indirectly detected with ^1H NMR through the exchange of the diene protons that are *cis* and *trans* to P(III). The $P,P=S$ ligands can become monodentate bound through P(III) and can then change sides followed by recoordination of the $P=S$ moiety. Since an equivalent complex of equal energy is most often obtained in this process, the steric and electronic properties of the ligand alone drive the exchange that is observed so that the effect of these properties on hemilability can be compared directly for this series of $P,P=S$ donor ligands. This system does not allow direct detection of the process where the $P=S$ dissociates then returns to the same position in a complex with the identical conformation.

For rhodium complexes of cod at slow exchange (assuming the ligand does not induce asymmetry across the square plane of the complex) one expects two olefin proton resonances and four methylene proton resonances. At fast exchange, which averages the protons *cis* and *trans* to P(III) (see Scheme 2), one expects a single olefin proton resonance and two methylene proton resonances. A series of ligands were examined in $[\text{Rh}(\text{cod})(P,P=S)][\text{SbF}_6]$ in CD_2Cl_2 . The complex of the smallest bite angle ligand dppm(S) (**1a**) does not exhibit *cis*–*trans* exchange on the NMR timescale over the temperature range accessible with CD_2Cl_2 , nor do complexes of the monosulfides of diphos (**1b**), (*S*)-BINAP (**1c**), or dppf (**1d**) implying that the barriers to *cis*–*trans* exchange for complexes of these ligands are $>19 \text{ kcal mol}^{-1}$. The complex formed with the larger chelate size ligand xantphos(S) (**1e**) has a decreased barrier to interconversion that can be observed in CD_2Cl_2 through the exchange of cod protons. Xantphos(S) was shown to have a barrier to *cis*–*trans* exchange of $15.1 \text{ kcal mol}^{-1}$ in CD_2Cl_2 . Only this phosphine monosulfide which forms a nine-membered chelate ring displays hemilability on the NMR timescale within the temperature range of CD_2Cl_2 . While the design of this system allowed us to determine which ligands undergo fast hemilabile processes over the temperature range studied, it was not practical for

Fig. 1. $P,P=S$ ligands.



Scheme 2. Hemilabile process for exchange of *cis* and *trans* positions relative to the cod ligand.

comparison of a range of chelate sizes and bite angles since the barrier to hemilability was too high for smaller bite angle ligands. We can only conclude that the largest bite angle ligand with little flexibility in the backbone has a decreased barrier to hemilability.

The principal insight provided by these experiments is that the barrier for hemilability is quite high for these ligands. Following the rearrangement pathway in Scheme 2, the free energies involved are schematically indicated in Fig. 2. The T–Y–T barrier E_3 is expected to be quite low (perhaps ~ 3 kcal mol⁻¹) [18–21] so that the barrier measured by *cis*–*trans* interconversion rate should be dominated by E_1 , the rate of conversion from κ^2 to κ^1 . Furthermore, one would expect the T–Y–T barrier to be similar for all of the κ^1 intermediates. The activation barrier for κ^1 to κ^2 (E_1 – E_2) would be expected to be quite small, so that the *cis*–*trans* barrier may be a composite of E_1 , E_2 , and E_3 , even though it would be dominated by E_1 . Since the *cis*–*trans* barriers are > 15 kcal mol⁻¹ they would appear to reflect the dominance of the κ^2 – κ^1 interconversion and thus the relative propensity for hemilability of the ligands.

In order to simplify the discussion, we have not yet addressed the effect of the conformations of the ligands and the nonrigidity of the conformations. The consequence of the metal–S–P angle tending to approach 90° produces conformations which tend to fold the ligand down, rather than away from the metal. This is illustrated in the crystal structure of the xantphos(S) complex (**1e**). The crystal structure revealed two interesting features (Fig. 3). The first is that the xanthene backbone is folded down in the solid structure similar to the folding observed in the previously reported bisphosphine palladium 1,1-dimethylallyl complex [22]. This is also reflected in the low T (< -60 °C) NMR spectrum in CD₂Cl₂ where twelve cod protons are seen. The xanthene backbone lies out of the plane of the complex, which creates enantiomeric conformations (see Scheme 3).

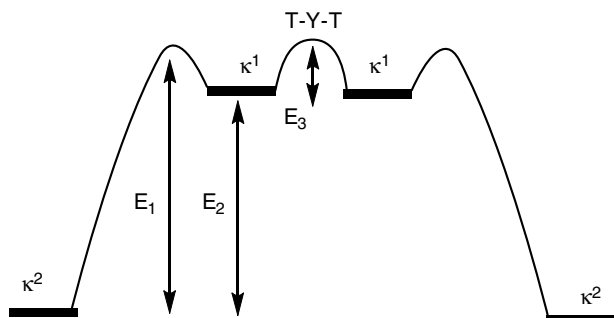


Fig. 2. Free energies involved in *cis*–*trans* interconversion.

For the xantphos(S) complex the exchange of enantiomers is slow on the NMR timescale at low temperatures and this is revealed by diastereotopic resonances in the cod ligand and the nonequivalent methyl resonances of the xantphos(S). At 10 °C, the backbone flips between the top and bottom of the complex sufficiently rapidly that it averages the resonances of cod protons above and below the plane of the complex. The methyl groups of the xantphos also average during this process. This flipping was found to have a barrier of 11.1 kcal mol⁻¹. The sides of the cod *cis* and *trans* to P(III) are inequivalent at 10 °C, which shows that exchange due to *cis*–*trans* exchange is slow at this temperature. We believe that this exchange of conformers occurs without scission of the S–Rh bond. This is consistent with averaging of conformers of most of the complexes at very low temperatures and lack of concomitant *cis*–*trans* interconversion.

The second feature of note in the crystal structure is the ligand bite angle. It is significantly contracted at 93.0° relative to the average bite angle 104.6° for the analogous bisphosphine. This same contraction is not observed with the dppm(S) complex where the bite angle of 89.3° (**1a**) (Fig. 3) is larger than the average bite angle $\sim 71.5^\circ$ for the analogous bisphosphine. Therefore, we can not simply predict the trend in bite angle of bisphosphine monosulfide ligands based on their bisphosphine bite angles. While the range of bite angles for a given bisphosphine is small for different metal geometries, the sulfide increases flexibility allowing the *P,P=S* ligands to better adapt to a metal geometry resulting in a much larger variation in bite angle with different metal complexes.

2.1.1. Backbone rigidity

The ligand backbones in the BINAP(S) and BIPHEP(S) are effectively rigid. In the BIPHEP(S) complex the chelation fixes the chirality of the biphenyl backbone such that one enantiomer of the ligand can be resolved [23]. The observation of four olefinic cod resonances at room temperature in the ¹H NMR of **1c** demonstrates that the barrier for interconversion is high.

Xantphos(S) has backbone constraints which allow for observable conformer exchange by NMR. The exchange occurs on the NMR timescale over the range of -80 °C to -40 °C. The barrier is sufficiently low for the cod rhodium derivative of xantphos(S), **1e**, so that averaged spectra are observed at R.T. in **1e** (barrier = 11.1 kcal mol⁻¹).

For the five and six-membered rings of dppm(S) and dppe(S) the barriers for interconversions of conformers are sufficiently low that averages are observed in the NMR. For example, for the methylene in **a**, the protons still

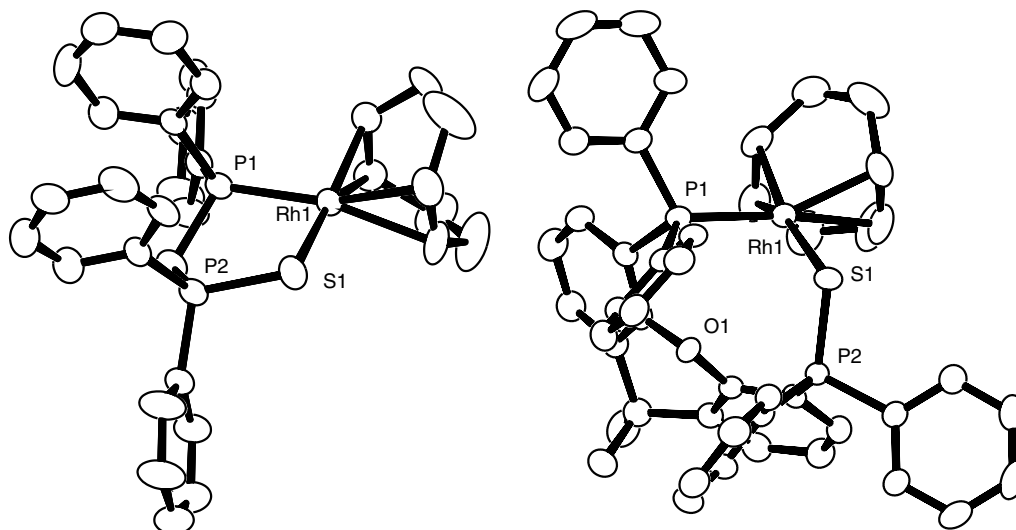
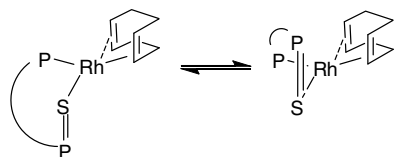


Fig. 3. ORTEP diagrams of the cations in $[\text{Rh}(\text{cod})(P,P=S)][\text{SbF}_6]$ (**1a**) and (**1e**). Bond distances (Å) and angles (°) for **1a**: Rh1–P1, 2.254(2); Rh1–S1, 2.344(2); P2–S1, 2.010(2); P1–Rh1–S1, 89.32(6); Rh1–S–P2, 107.01(9). Bond distances and angles for **1e**: Rh1–P1, 2.331(1); Rh1–S1, 2.400(1); P2–S1, 2.004(1); P1–Rh1–S1, 92.99(4); Rh1–S–P2, 108.47(5).



Scheme 3. Conformational interchange in $P,P=S$ ligands.

appear equivalent at $-80\text{ }^\circ\text{C}$, suggesting a very low barrier ($<10\text{ kcal mol}^{-1}$) for interconversion of ring conformations. One should note that the dppe backbone could have more than one low energy conformation, although one is probably preferred and induced by the chirality of the P–Rh–S–P moiety.

Even though the ring size is larger, the flexibility available in the ferrocenyl unit of dppf(S) allows rapid interconversion of the enantiomers of **1d** at ambient temperature. The enantiomer interconversion is slowed at $-20\text{ }^\circ\text{C}$ and two diastereomeric conformers are observed in the ^{31}P NMR in a ratio of 20:1.

2.1.2. Other possible mechanisms consistent with the observations of enantiomer interconversion

It is possible, however, that the backbone flip could involve dissociation of $\text{P}=\text{S}$ in a hemilabile process that is consistent with the observed behavior if T–Y–T exchange were slow. A planar to tetrahedral conversion could also occur, but the electronic configuration of these d^8 complexes would make this a highly energetic pathway. The possible conversion into a nonrigid five-coordinate complex by coordination of solvent or another ligand is probably the most likely alternative. For the rhodium complexes **1b–1e** the NMR spectra did not show an increase in rate upon changing the solvent to acetone- d_6 . In general, these observations and our interpretations, such

as those shown in Scheme 2, are consistent with those found for other $[\text{Rh}(\text{cod})(\text{bidentate ligand})]^+$ complexes [24], but the relative barrier heights are different. The consequences of the conformational interconversions will be discussed in more detail later in the context of palladium allyl complexes.

2.2. $[\text{Pd}(\eta^3\text{-C}_3\text{H}_5)(P,P=S)][\text{SbF}_6]$ complexes (**2**)

To further examine fluxional processes of complexes of $P,P=S$ ligands a series of complexes $[\text{Pd}(\eta^3\text{-C}_3\text{H}_5)(P,P=S)][\text{SbF}_6]$ (**2**) was prepared using the same bisphosphine monosulfides. The complex $[\text{Pd}(\eta^3\text{-C}_3\text{H}_5)(\text{dppm}(\text{S}))][\text{SbF}_6]$ (**2a**) has only one chiral center at the metal so only one pair of enantiomers is possible. The phosphorus atoms cannot exchange with each other so the ^{31}P NMR exhibits two sharp doublets at all temperatures (see Fig. 4).

The ^1H NMR was observed over the temperature range $-75\text{ }^\circ\text{C}$ to $58\text{ }^\circ\text{C}$ in CD_2Cl_2 or CDCl_3 depending upon the temperature (see Fig. 5). At low temperature there are five allyl protons and two protons from the ligand backbone. In this complex the protons on the backbone are diastereotopic and effectively report on their relationship to the central proton of the allyl. The backbone protons will exchange with each other if a fluxional process is interconverting enantiomers. Two of the processes discussed above, $\eta^3\text{-}\eta^1\text{-}\eta^3$ exchange of the allyl ligand and migration of the phosphorus, can interconvert the enantiomers and

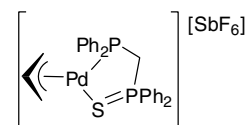


Fig. 4. Structure of $[\text{Pd}(\eta^3\text{-C}_3\text{H}_5)(\text{dppm}(\text{S}))][\text{SbF}_6]$ (**2a**).

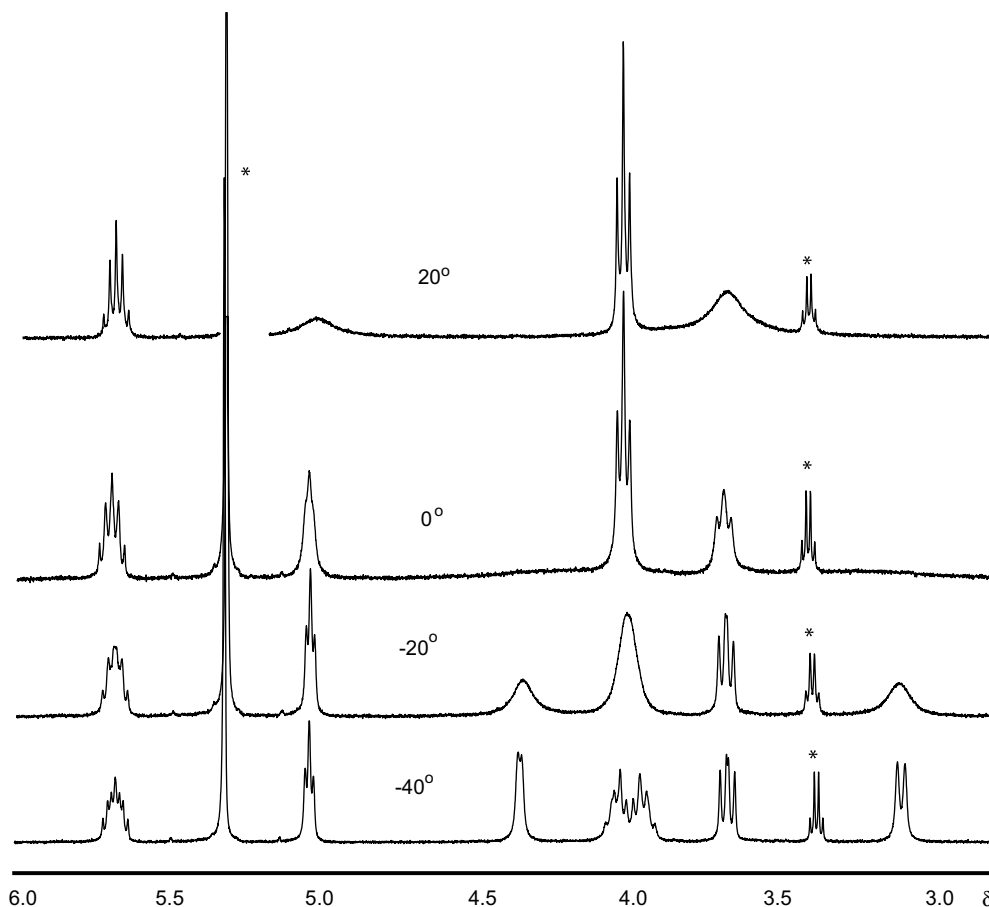


Fig. 5. The ^1H DNMR of $[\text{Pd}(\eta^3\text{-C}_3\text{H}_5)(\text{dppm}(\text{S}))][\text{SbF}_6]$ (**2a**) in CD_2Cl_2 . Impurities are indicated by an asterisk.

therefore will exchange the backbone protons. These processes are slow at -60°C according to the ^1H NMR data. On increasing the temperature, the backbone proton resonances and two of the terminal allyl proton resonances begin to broaden at -40°C , while two of the terminal allyl resonances remain sharp up to -10°C but are broad at 0°C , evidence which suggests two distinct fluxional processes with different barriers. The first process is attributable to an $\eta^3\text{-}\eta^1\text{-}\eta^3$ rearrangement of the allyl ligand and, as a result of the *trans* effect, we expect the η^1 -bound allyl to be *cis* to phosphorus and therefore only the *cis* protons will exchange with one another. The *trans* protons will return to the same *syn* or *anti* position when the allyl returns to η^3 coordination. Only this process would result in the observation of four allyl proton resonances in an averaged spectrum, where the phosphorus migration would result in three allyl proton resonances.

Identification of the second fluxional process was more difficult. At 58°C , all of the terminal allyl resonances are broad. It was not initially clear whether all four of the allyl resonances were exchanging with one another or if there were two separate resonances which were not exchanging with each other. This problem was solved by ^{13}C NMR. At 25°C , the terminal allyl carbon resonances are broad, which implies that there is exchange of the positions *cis*

and *trans* to phosphorus. This allows us to rule out a mechanism where the formation of an η^1 complex *trans* to phosphorus is exchanging the *syn*, *trans* and *anti*, *trans* protons. Therefore, it can be concluded that the $\eta^3\text{-}\eta^1\text{-}\eta^3$ exchange causes averaging of the *cis*, *syn* and *cis*, *anti* protons, while the second fluxional process exchanges the *cis* protons with the corresponding *trans* protons. The combination of these fluxional processes averages all four terminal allyl protons. The second fluxional process is consistent with phosphorus migration and it is also consistent with migration of the η^1 -allyl to the position *trans* to phosphorus but this is expected to be unfavorable since it would be moving from a position that is *trans* to a weaker *trans* effect ligand.

Changing the solvent to acetone- d_6 results in the observation of two isomers in the ^{31}P NMR which indicates that coordination of acetone to the palladium complex is taking place. The exchange of the allyl protons acetone- d_6 solution appears to occur with similar barriers to those observed in CD_2Cl_2 solution, which further suggests that coordination of an acetone does not materially affect the rate of the allyl exchange.

With these data in hand, the other complexes in the series were examined. In CDCl_3 at higher temperature limit for the solvent complexes **2b** and **2d** showed some broadening suggesting a barrier to *syn-anti* exchange at the

position *cis* to phosphorus of approximately 18 kcal mol⁻¹. In acetone-d₆ solution, there is a decrease in the barrier to both the *cis* to phosphorus *syn-anti* exchange, and *cis-trans* exchange for **2b** whereas changing solvent to acetone-d₆ has no effect on the barrier to those processes for complexes **2a** and **2d**. The more coordinating solvent is likely to encourage an allyl hapticity change as well as acceleration of *cis-trans* exchange via an associative mechanism. The fact that this does not occur in every case suggests that the ligand bite angle or the electronic properties can affect these exchange processes.

Pregosin and co-workers have investigated the dynamics of some 1,3-substituted allylpalladium complexes with (*P,S*) donors where the sulfur is within a thioether linkage [25]. In that case, the allyl substituents effectively prevent the *syn-anti* exchange observed here, but do not necessarily prevent *cis-trans* exchange [26]. Of particular relevance is our previously published analysis of rearrangements of the BINAP(S) allyl analogue, **2c** [16]. A saturation transfer experiment showed that allylic termini interconversion occurs 1.4 times faster than $\eta^3-\eta^1-\eta^3$ exchange at 62 °C. In this case, exchange due to hemilability appears to occur with a slightly lower barrier than the $\eta^3-\eta^1-\eta^3$ process.

2.2.1. Effect of chelate ring size and bite angle

Average bite angles for *P,P* ligands have been reported [27] and selected values are presented in Table 1. The bite angles of *P,P=S* ligands do not necessarily follow the same trend as *P,P* ligands as is illustrated in the small xantphos(S) bite angle in complex **1e** and the large dppm(S) bite

angle in **1a** relative to the average bite angles of their *P,P* analogues. The bite angles of known *P,P=S* complexes are presented in Table 1 in order to illustrate the large variation in bite angle that is possible for a given *P,P=S* ligand. This variation is illustrated in the bite angles given for (*S*)-BINAP(S) complexes ranging from 89.11° to 100.45°.

2.3. [Pd(C(H)(PPh₂)(P(S)Ph₂)₂)Cl₂] (**3**)

The challenge to observing hemilability by NMR is that often the complex is unchanged upon dissociation and reassociation of the labile donor. Other fluxional processes within the complex studied must also be considered and they may be difficult to distinguish from hemilability. Therefore, we initially investigated this palladium system where the only possible fluxional process was hemilability. One approach to the observation of ligand dissociation and reassociation is the observation of exchange between bound and free ligands. Since hemilability is inherently an intramolecular process, this requires that both the bound and free donor be contained within the same ligand. The first complex studied was [Pd(C(H)(PPh₂)(P(S)Ph₂)₂)Cl₂] (**3**), shown in Fig. 6, which potentially allows observation of the hemilabile nature of the ligand. Upon coordination of the metal, the ligand becomes chiral, so *P=S* exchange inverts the ligand chirality resulting in the exchange of enantiomers. Furthermore, after breaking of the Pd-S bond, the three-coordinate intermediate has the possibility of recoordination with either of the sulfur donors, which would provide a method of detection of the bond-breaking (see Scheme 4). Therefore, the readily observed resonances that are exchanged by this process are the ³¹P NMR resonances of the *P=S* moiety. If exchange of the *P=S* moiety bound to palladium with the free *P=S* moiety is slow on the NMR timescale, observation of three doublets of doublets would be expected, since the three phosphorus nuclei would be inequivalent and would all be coupled to one another. If exchange were fast on the NMR timescale, two resonances would be observed, a triplet for P(III), and a doublet for the two equivalent *P=S* moieties. This exchange could also result from an associative mechanism (see below).

The initial observation was that at 20 °C, the P(III) resonance was a near sharp triplet (δ 51, $J = 21$ Hz) as expected for the fast exchange condition. The *P=S* resonances at δ 43 and δ 35 were extremely broad and the coupling could not be observed. Upon cooling to 0 °C, one of the *P=S* resonances shifted significantly to δ 63,

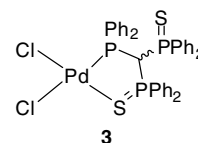


Fig. 6. Hapticity observed for [Pd(HC(PPh₂)(P(S)Ph₂)₂)Cl₂].

Table 1
Known bite angles for *P,P* and *P,P=S* ligands

<i>P,P</i>	Pd/ <i>P,P=S</i>		Rh/ <i>P,P=S</i>	M/ <i>P,P=S</i>
	β^a	β	β	β
Ph ₂ PCH ₂ PPh ₂	71.53	95.74 ^b 91.21 ^c	89.3	
Ph ₂ P(CH ₂) ₂ PPh ₂	82.55	90.17 ^d		86.4 ^e
BIPHEP	91.63 ^f	92.85 ^g		
BINAP(S)	92.77	92.83 ^h 89.11 ⁱ 99.01 ^j 100.45 ^k		
Dppf	98.74			85.75 ^l
Xantphos	104.64		93.0	

^a Average bite angles in Cambridge Crystallographic Database [27].

^b [Pd(η^3 -C₃H₅)-(dppm(S))][OtF] [28].

^c [Pd(II)(dppm(S))₂] [29].

^d [Pd(diphos(S))Cl₂], FOXGIL.

^e [Ru(η^6 : η^1 -NMe₂-C₆H₄-C₆H₄PCy₂)(diphos(S))][SbF₆] [30].

^f [Rh(2-(4-*tert*-butyl-phenyl)-8-methoxy-1,8-dimethyl-bicyclo-[2.2.2]octa-2,5-diene)(biphep)][SbF₆] [23].

^g [Pd(η^3 -C₃H₅)(biphep(S))][SbF₆] [16].

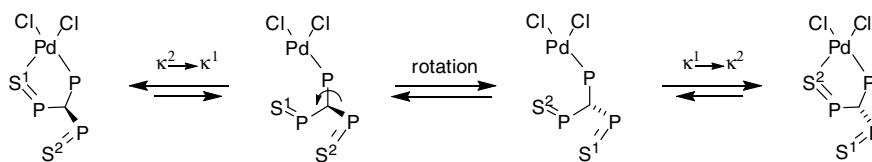
^h [Pd(η^3 -C₃H₅)(*S*)-BINAP(S)][BF₄] [31].

ⁱ [Pd(*S*)-BINAP(S)Cl₂] [31].

^j [Pd(η^3 -cinnamylallyl)(*S*)-BINAP(S)][SbF₆] [16].

^k [Pd-(η^3 -1,1-dimethylallyl)(*S*)-BINAP(S)][SbF₆] [16].

^l [Pd(Me₈-dppf(S))Cl₂] [32] m. Calculated value [27].



Scheme 4. A hemilabile mechanism for P=S exchange in 3.

while the other shifted only slightly to δ 34. The center resonance of the P(III) triplet also broadened while the outer resonances remained sharp. Further cooling yields a spectrum where all three resonances are sharp at -60 °C. One doublet of doublets (δ 52, $J = 47$ Hz, $J = 5$ Hz) and two doublets (δ 64, $J = 47$ Hz; δ 34, $J = 5$ Hz) are observed as expected for P=S exchange that is slow on the NMR timescale. The value of the coupling of the P(III) nucleus to one of the P=S nuclei must be negative while the other is positive to give the average coupling of 21 Hz for the P(III) triplet at high temperature. Even at -80 °C, the coupling between the two P=S phosphorus nuclei is not observed. Assuming slow exchange at -60 °C, the barrier to P=S exchange was determined to be 12.0 kcal mol $^{-1}$ by line broadening analysis.

Even though one might hope that this provided a definitive demonstration of hemilability, one disadvantage to this system is that the second P=S moiety may encourage an exchange process equivalent to hemilability through an associative mechanism of P=S exchange that could decrease the barrier to exchange relative to complexes of ligands such as $\text{Ph}_2\text{PCH}_2\text{P}(\text{S})\text{Ph}_2$ that do not have such an associative mechanism available to them. In fact, it is more probable that exchange in this system does not involve a dissociative mechanism, but involves an associative process wherein a five-coordinate fluxional intermediate (Fig. 7) is formed and this allows exchange of the two P=S moieties.

2.4. $[\text{Pd}(\eta^3\text{-C}_3\text{H}_5)(\text{HC}(\text{PPh}_2)(\text{P}(\text{S})\text{Ph}_2)_2)][\text{SbF}_6]$ (4)

The X-ray crystal structure of 4 (Fig. 8) showed that the ligand was P,S bound (Fig. 9), and both the *endo* and *exo* orientation of the allyl relative to the uncoordinated P=S moiety were observed as a disorder in the crystal. These crystals did not indicate the presence of two isomers by ^1H and ^{31}P NMR spectroscopy in CD_2Cl_2 owing to the rapid interconversion of the two isomers by the dissociation of the bound P=S and association of the unbound P=S, either through an associative or a dissociative mechanism. Assuming the position of the P(III) relative to the

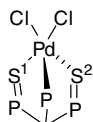


Fig. 7. An intermediate five-coordinate complex in an associative mechanism for P=S exchange in 3.

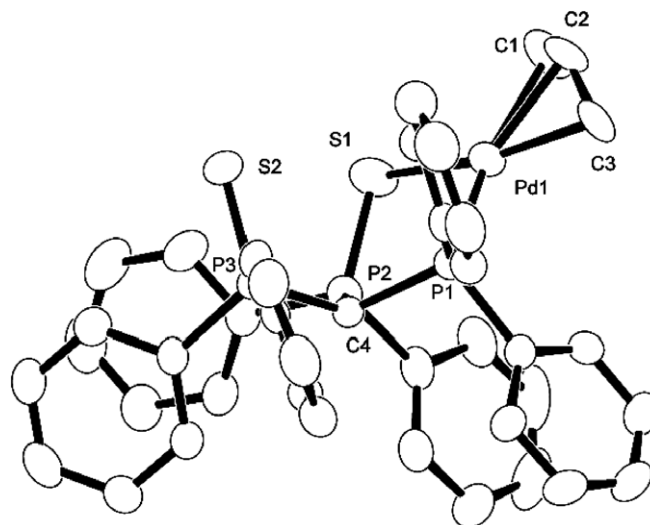
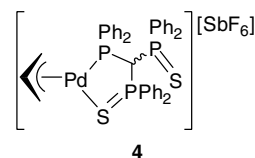
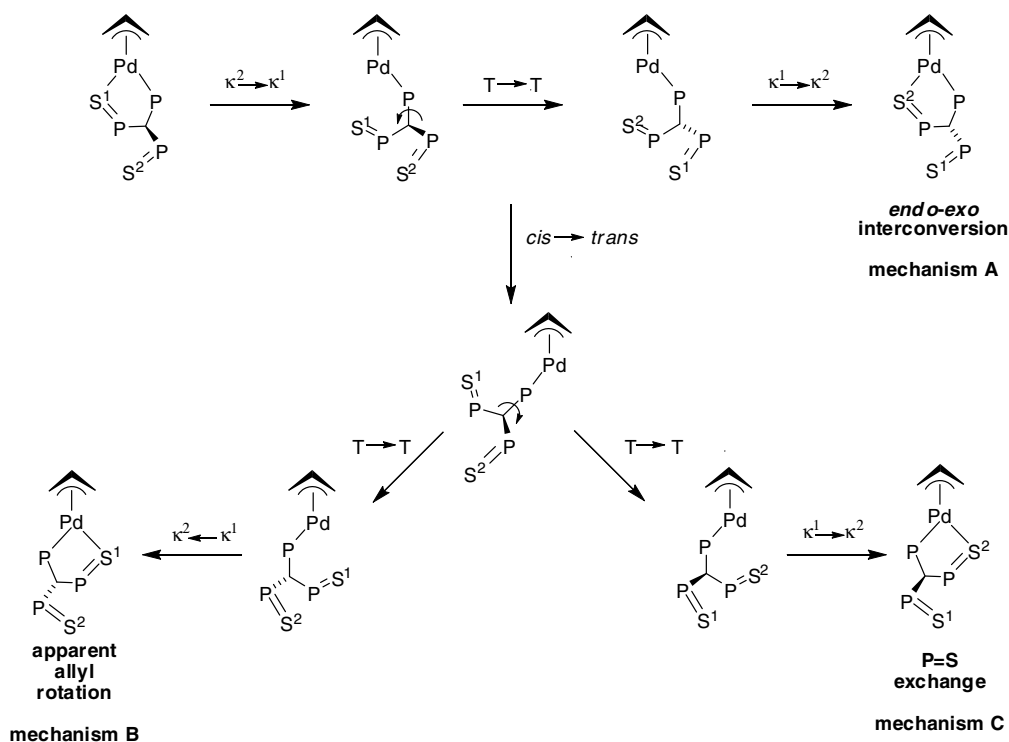


Fig. 8. An ORTEP diagram of a cation in $[\text{Pd}(\eta^3\text{-C}_3\text{H}_5)(\text{HC}(\text{PPh}_2)(\text{P}(\text{S})\text{Ph}_2)_2)][\text{SbF}_6]$ (4). Bond distances (Å) and angles (°) for 4: Pd1–P1, 2.280(2); Pd1–S1, 2.336(2); P2–S1, 2.000(2); P3–S2, 1.942(2); Pd1–C1, 2.191(6); Pd1–C3, 2.132(6); P1–Pd1–S1, 94.78(5).

Fig. 9. The hapticity of $[\text{Pd}(\eta^3\text{-C}_3\text{H}_5)(\text{HC}(\text{PPh}_2)(\text{P}(\text{S})\text{Ph}_2)_2)][\text{SbF}_6]$ (4).

allyl does not change this process would also interconvert the *exo* and *endo* isomers (see Scheme 5, mechanism A). Variable temperature NMR study shows that this isomer exchange is fast at -60 °C. If we first examine this hemilabile ligand exchange, assuming all other fluxional processes to be slow, we would expect each P=S to be averaged between the free and bound position, whereas the two P=S moieties will remain diastereotopic. When we observe the ^{31}P NMR of this complex there are two P=S phosphorus nuclei that are inequivalent at lower T (< -20 °C) which is consistent with mechanism A (Scheme 5) being the only fast process under these conditions. At high T (> 0 °C), the P=S resonances are averaged, so a second fluxional process is responsible for the exchange of the P=S moieties. Identification of this second fluxional process is discussed with the assumption that isomer exchange via mechanism A in Scheme 5 is fast under the conditions used to observe the second fluxional process.

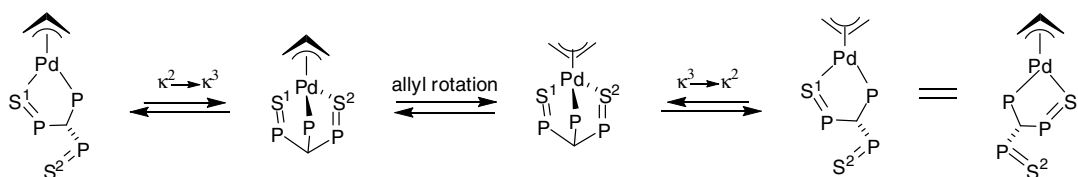


Scheme 5. Hemilabile mechanisms for *endo-exo* interconversion (A), apparent allyl rotation (B), and P=S exchange (C).

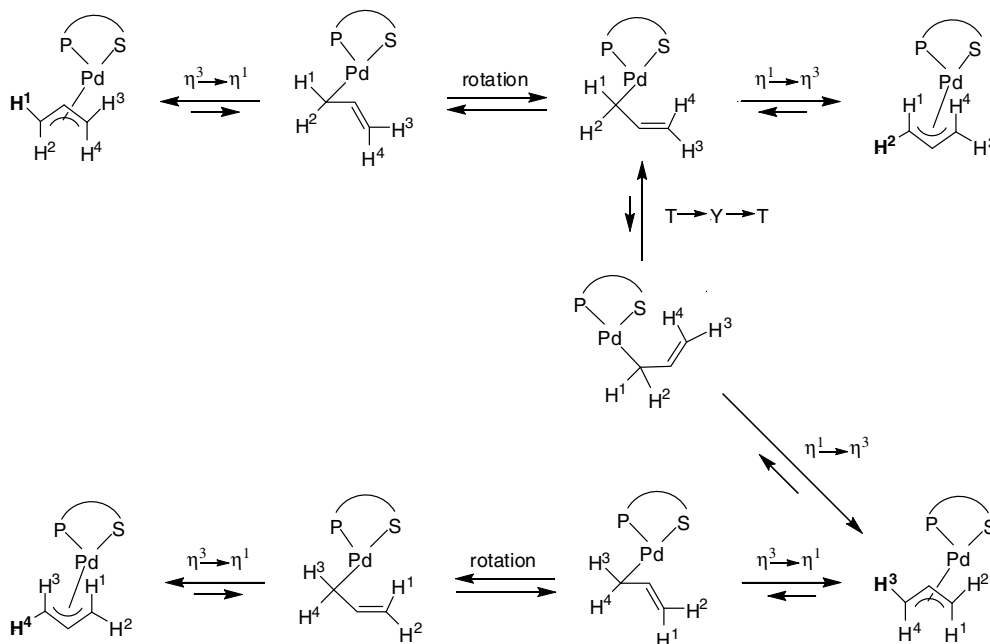
We will first consider the second process as a result of hemilability in the absence of allyl exchange. *Endo-exo* exchange is necessary to average the P=S resonances and can occur through an apparent allyl rotation resulting from ligand rearrangement (Scheme 5, mechanism B). This requires the bound P=S to dissociate and a T-shaped intermediate to form. The P(III) can then return to the same position or move to the position where the P=S was bound whereupon the P=S can then coordinate in the position that the P(III) has just left. The net result of this process, with retention of ligand configuration, is an allyl rotation where the terminal allyl carbon *trans* P becomes *trans* to S, and *endo-exo* isomerism also occurs, but the orientation of the terminal allyl protons, *syn* or *anti* relative to the central allyl proton, is retained. This process, coupled with fast free and bound P=S exchange, will average the P=S resonances. This is depicted in Scheme 5 where the P=S exchange (mechanism C) is the sum of an isomer exchange (mechanism A) and an apparent allyl rotation (mechanism B). ^1H NMR will show exchange of *cis* and *trans* protons but not *syn* and *anti* protons if this process is responsible for P=S exchange.

Apparent allyl rotation can also occur via pseudorotation (Scheme 6). For a four-coordinate palladium complex, there is no low energy pathway available by which allyl rotation can occur, but coordination of the free P=S moiety would give a five coordinate complex which effectively allows a pathway for allyl rotation [33–37]. This mechanism is not distinguishable by NMR from the hemilabile ligand dissociation mechanism for apparent allyl rotation.

A fluxional allyl process involving an η^3 – η^1 – η^3 mechanism could also be responsible for P=S exchange (Scheme 7). In this process, the allyl becomes η^1 then returns to η^3 either *endo* or *exo* relative to the unbound P=S. This process may also result in *cis-trans* exchange, but this mechanism requires the η^1 -allyl to move from a *cis* position to the more labile *trans* position relative to P(III), the higher *trans* effect donor, so it is unlikely to occur in this system. *Endo-exo* exchange via the formation of an η^1 -allyl results in the exchange of the *syn* and *anti* protons on the σ bound carbon through a C–C bond rotation. Therefore, we can distinguish this mechanism from the previous two mechanisms by ^1H NMR. If either or both sets of the *syn* and *anti* protons exchange, then an η^3 – η^1 – η^3 mechanism



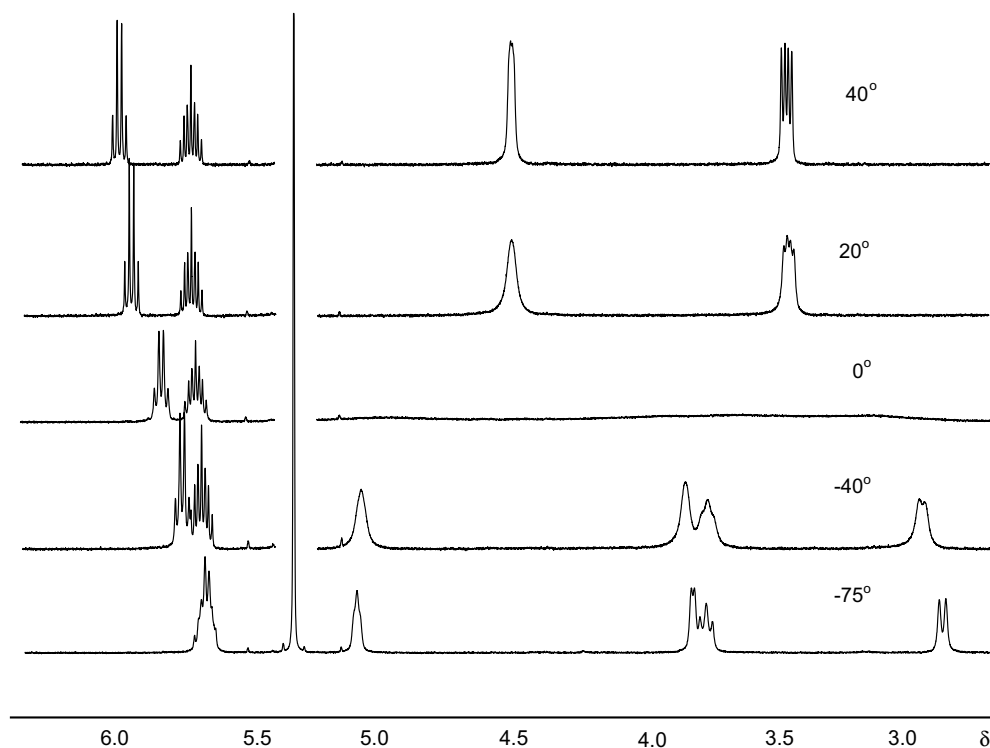
Scheme 6. Isomer interconversion via an allyl pseudorotation.

Scheme 7. Isomer and *syn-anti* interconversion via an η^3 - η^1 - η^3 isomerization.

must be involved, but if no *syn-anti* exchange is observed than an η^3 - η^1 - η^3 mechanism can not be involved in P=S exchange.

A variable temperature ^1H NMR study shows five allyl resonances at low temperature ($T < -40^\circ\text{C}$) and three allyl resonances at high temperature ($T > 0^\circ\text{C}$), as shown in Fig. 10. This rules out the η^3 - η^1 - η^3 exchange with only

the *trans* carbon dissociating, but does not rule out dissociation of the *cis* and *trans* carbons at competitive rates. It was therefore necessary to determine if the *cis* and *trans* positions become equivalent at high temperatures while the *syn* and *anti* positions remain inequivalent, or if the reverse is true. This was accomplished using $^1\text{H}\{^{31}\text{P}\}$ NMR and a summary of the allyl resonances is given in Table 2 [38].

Fig. 10. The ^1H DNMR of $[\text{Pd}(\eta^3\text{-C}_3\text{H}_5)(\text{HC}(\text{PPh}_2)(\text{P}(\text{S})\text{Ph}_2))][\text{SbF}_6]$ in CD_2Cl_2 .

The $^1\text{H}\{^{31}\text{P}\}$ spectrum at 40 °C shows clearly which protons are exchanging. Two doublets remain for the terminal allyl protons. The resonance at δ 3.48 is a doublet with $^3J_{\text{HH}} = 13.1$ Hz. This is consistent with exchange of the *cis*, *anti* and *trans*, *anti* protons. At low temperature, the apparent triplets are assigned as the *trans* protons because they exhibit phosphorus coupling that is of similar magnitude to the central proton coupling. The doublet with the larger coupling constant at δ 2.87 is assigned to an *anti* proton while the doublet at δ 3.80 is assigned to a *syn* proton. If the *trans*, *anti* and *cis*, *anti* resonances average, we expect a doublet of doublets where $^3J_{\text{HH}} = 13.1$ Hz, and $J_{\text{PH}} \sim 6$ Hz since we assume the phosphorus coupling to the *cis* proton to be close to zero. In fact we observe $^3J_{\text{HH}} = 13.1$ Hz, and $J_{\text{PH}} = 6.9$ Hz. The larger value (>5.5 Hz) of phosphorus coupling suggests some contribution from a *cis* P,H coupling.

These data show that *cis*, *anti* and *trans*, *anti* protons are exchanging and the *cis*, *syn* and *trans*, *syn* protons are exchanging. This is consistent with the first two proposed mechanisms, P(III) migration and associative pseudorotation. It rules out any contribution from $\eta^3\text{-}\eta^1\text{-}\eta^3$ allyl exchange. We can therefore conclude that $\eta^3\text{-}\eta^1\text{-}\eta^3$ allyl process is slow at 40 °C where the two terminal allyl resonances are nearly sharp.

We subsequently recorded the NMR spectra of the complex in a coordinating solvent, acetone- d_6 over the temperature range -75 °C to 60 °C. The NMR data in acetone- d_6 are very similar to those in CD_2Cl_2 , the four terminal allyl proton resonances begin broadening at -40 °C and sharpen into two resonances by 60 °C and, in the ^{31}P NMR spectrum, the two P=S resonances begin broadening at -40 °C, and sharpen into one resonance by 60 °C. This is consistent with the CD_2Cl_2 data where the ^1H and ^{31}P resonances begin to broaden at -40 °C and are nearly sharp at 40 °C. Therefore, in each solvent the low temperature limit for fast exchange of the positions *cis* and *trans* to P is between 40 °C and 60 °C, while the high temperature limit for slow exchange of those positions is between -60 °C and -40 °C. Further, in each solvent the barriers to exchange of the ^{31}P resonances are similar to the barriers for exchange of the ^1H resonances. This suggests the same

process that exchanges the allyl resonances is also exchanging the P=S resonances and the similarity of the data for the two solvents suggests that there is not likely to be any significant effect of solvent coordination on the exchange processes that are being observed.

In summary, these observations would suggest that the most likely mechanism is conversion to a κ^3 intermediate followed by pseudorotation of the five-coordinate intermediate and finally dissociation of a P=S to produce an isomerized κ^2 complex as was shown in Scheme 6.

2.5. Deprotonation of $[\text{Pd}(\eta^3\text{-C}_3\text{H}_5)\text{-}(\text{HC}(\text{PPh}_2)(\text{P}(\text{S})\text{Ph}_2)_2)][\text{SbF}_6]$ to yield $[\text{Pd}(\eta^3\text{-C}_3\text{H}_5)(\text{C}(\text{PPh}_2)(\text{P}(\text{S})\text{Ph}_2)_2)]$ (5)

In order to confirm the mechanism for P=S exchange involved a κ^3 intermediate, the backbone proton of the $\text{P,P}=\text{S,P}=\text{S}$ ligand in **4** was removed to give a planar geometry of the ligand that would prevent coordination of the unbound P=S. $[\text{Pd}(\eta^3\text{-C}_3\text{H}_5)(\text{HC}(\text{PPh}_2)(\text{P}(\text{S})\text{Ph}_2)_2)][\text{SbF}_6]$ was deprotonated with two equivalents of triethylamine. The deprotonated complex exists as a set of enantiomers and, as expected, three doublets of doublets are present in the ^{31}P NMR and there are five distinct allyl protons in the ^1H NMR. The deprotonation of the ligand prevents the fluxional processes involving the $\text{P,P}=\text{S}$ ligand which exchange the allyl protons. This lends further support to Scheme 6 being the preferred pathway since the geometry does not permit the formation of a κ^3 intermediate (see Fig. 11).

2.6. Comparison of P=S exchange in allyl and dichloride complexes

In the ^{31}P NMR spectrum of the allyl complex **4** at -75 °C, only one set of resonances is observed despite the fact that the *cis*–*trans* exchange is slow. Therefore, *endo*–*exo* exchange between free and bound P=S moieties is still occurring on the NMR timescale. It is important to distinguish here between the low temperature process that averages the environment of each P=S moiety but retains their diastereotopicity, *endo*–*exo* isomerism which is fast at -40 °C, and *cis*–*trans* isomerism which inverts the chirality at palladium and, coupled with the *endo*–*exo* isomerism, exchanges the P=S moieties (Scheme 8). Broadening of the P=S resonances upon cooling from -40 °C to -60 °C suggests the exchange of diastereomers is becoming slow. In contrast, in the dichloride simple exchange between free and bound P=S does produce the same aver-

Table 2
 ^1H NMR of **3**

Spectrum	Δ	J (Hz)	H
^1H , -60 °C	5.69	apparent tt, ~ 7.1 , ~ 13.1	Central
	5.06	apparent t, ~ 7.1	<i>trans</i> , <i>syn</i>
	3.80	Br d, ~ 6.6	<i>cis</i> , <i>syn</i>
	3.73	dd, 13.2 (H,H) 11.0 (H,P)	<i>trans</i> , <i>anti</i>
	2.87	d, 12.9	<i>cis</i> , <i>anti</i>
^1H , 40 °C	5.66	tt, 7.1, 13.1	Central
	4.48	Br dd, 7.1 (H,H)	<i>cis/trans</i> , <i>syn</i>
	3.42	dd, 13.1 (H,H) 6.9 (H,P)	<i>cis/trans</i> , <i>anti</i>
$^1\text{H}\{^{31}\text{P}\}$, 40 °C	5.76	tt, 7.1, 13.1	Central
	4.53	d, 7.1	<i>cis/trans</i> , <i>syn</i>
	3.48	d, 13.1	<i>cis/trans</i> , <i>anti</i>

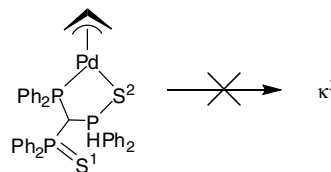
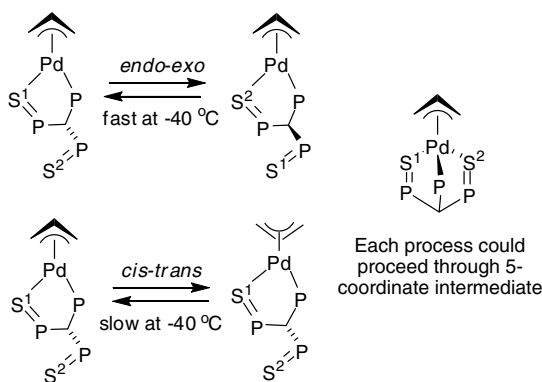


Fig. 11. Complex **5** obtained by deprotonation of **4** remains κ^2 .

Scheme 8. *Endo-exo* and *cis-trans* exchange in the cation of **4**.

age environment for the P=S moieties because the only chirality in the complex is associated with the ligand. This means there is an exchange of enantiomers, not diastereomers, so no additional process is necessary to make the P=S resonances equivalent.

Since there are two P=S resonances for the dichloride at $-60\text{ }^{\circ}\text{C}$, free and bound exchange is slow at this temperature. This demonstrates that the barrier to free and bound P=S exchange is smaller in the allyl complex than in the dichloride complex, as the barrier for exchange in the dichloride is $12.0\text{ kcal mol}^{-1}$, while in the allyl complex the barrier must be less than 11 kcal mol^{-1} . We also know that the barrier to $\eta^3\text{-}\eta^1\text{-}\eta^3$ exchange is much lower for **2a** than for the complexes of *P,P=S,P=S* ligands. In contrast, the barrier to the *cis-trans* exchange process is higher in **2a** and therefore a free P=S moiety is not necessary for the observed *cis-trans* exchange process but it does decrease the barrier to the process in some way. Therefore, this further suggests an associative mechanism leading to allyl pseudorotation may be operating in the *P,P=S,P=S* complexes.

3. Conclusions

Hemilability and allyl exchange mechanisms of palladium and rhodium complexes of *P,P=S* ligands have been studied by variable temperature NMR. Larger bite angle and larger chelate ring ligands were found to have lower barriers for hemilability.

4. Experimental

4.1. General methods

All synthetic manipulations were performed under a nitrogen atmosphere using standard Schlenk techniques. CH_2Cl_2 was dried by distillation over CaH_2 and thf was dried by distillation over Na and benzophenone. $[\text{Rh}(\text{cod})\text{Cl}]_2$ [39], $[\text{Pd}(\eta^3\text{-C}_3\text{H}_5)\text{Cl}]_2$ [40], complexes **1a** [28], **1c** [15], and $[\text{HC}(\text{PPh}_2)(\text{P}(\text{S})\text{Ph}_2)_2]$ [41] were prepared by published methods. The known *P,P=S* ligands **a** [42], **b** [43], **c** [15], **d** [44], were prepared in analogy to the published method [30] and characterization data was in accord

with that previously reported. The complex **2a** has previously been prepared with other counter ions [45]. NMR spectra were recorded on Bruker 400 or 500 MHz instruments and the chemical shifts reported in ppm relative to TMS by calibration with reference to solvent resonances.

4.2. General procedure for preparation of $[\text{Rh}(\text{cod})(\text{P,P=S})][\text{SbF}_6]$ (**1**)

$[\text{Rh}(\text{cod})\text{Cl}]_2$ (0.1 mmol) was dissolved in CH_2Cl_2 (10 mL) and one equivalent of the appropriate *P,P=S* ligand was added to the solution. NaSbF_6 (0.22 mmol) was then added and the mixture was stirred for 6 h at R.T. The solution was filtered through Celite and the solvent removed by rotary evaporation.

4.2.1. $[\text{Rh}(\text{cod})(\text{Ph}_2\text{PCH}_2\text{P}(\text{S})\text{Ph}_2)][\text{SbF}_6]$ (**1a**)

^1H NMR (400 MHz, CD_2Cl_2 , $22\text{ }^{\circ}\text{C}$) δ : 7.66–7.37 (20H, m, Ph-*H*); 5.81 (2H, m, cod-CH); 3.98 (2H, dd, PCH_2 , $^2J_{\text{PH}} = 10\text{ Hz}$, $^1J_{\text{PH}} = 10\text{ Hz}$); 3.57 (2H, m, cod-CH); 2.57–2.32 (6H, m, cod- CH_2); 2.24–2.17 (2H, m, cod- CH_2). ^{31}P NMR (162 MHz, CD_2Cl_2) δ : 57.3 (d, P=S, $J_{\text{PP}} = 51.8\text{ Hz}$); 39.8 (dd, P(III), $J_{\text{PP}} = 51.8\text{ Hz}$, $J_{\text{RHP}} = 148.6\text{ Hz}$).

4.2.2. $[\text{Rh}(\text{cod})(\text{Ph}_2\text{P}(\text{CH}_2)_2\text{P}(\text{S})\text{Ph}_2)][\text{SbF}_6]$ (**1b**)

^1H NMR (500 MHz, CD_2Cl_2 , $22\text{ }^{\circ}\text{C}$) δ : 7.88 (4H, m, Ph-*H*); 7.77 (2H, m, Ph-*H*); 7.69–7.51 (14H, m, Ph-*H*); 5.48 (2H, m, cod-CH); 3.52 (2H, m, cod-CH); 3.04 (2H, m, PCH_2); 2.79 (2H, m, PCH_2); 2.49 (2H, m, cod- CH_2); 2.41 (2H, m, cod- CH_2); 2.33 (2H, m, cod- CH_2); 2.15 (2H, m, cod- CH_2). ^{31}P NMR (162 MHz, CD_2Cl_2) δ : 41.3 (dd, P=S, $J_{\text{PP}} = 15.1\text{ Hz}$, $^1J_{\text{RHP}} = 3.5\text{ Hz}$); 19.2 (dd, P(III), $J_{\text{PP}} = 15.1\text{ Hz}$, $^1J_{\text{RHP}} = 148.6\text{ Hz}$). ^{13}C NMR (126 MHz, CD_2Cl_2) δ : 133.7 (2C, d, Ph-C, $J_{\text{PC}} = 3.0\text{ Hz}$); 133.4 (4C, d, Ph-C, $J_{\text{PC}} = 10.6\text{ Hz}$); 131.5 (2C, d, Ph-C, $J_{\text{PC}} = 2.5\text{ Hz}$); 131.4 (4C, d, Ph-C, $J_{\text{PC}} = 10.4\text{ Hz}$); 130.0 (2C, d, Ph-CP, $J_{\text{PC}} = 44.3\text{ Hz}$); 129.6 (4C, d, Ph-C, $J_{\text{PC}} = 12.6\text{ Hz}$); 129.0 (4C, d, Ph-C, $J_{\text{PC}} = 10.1\text{ Hz}$); 126.7 (2C, d, Ph-CP, $J_{\text{CP}} = 82.7\text{ Hz}$); 107.5 (2C, dd, cod-CH, $J_{\text{PC}} = 11.0\text{ Hz}$, $J_{\text{RhC}} = 6.5\text{ Hz}$); 80.4 (2C, dd, cod-CH, $J_{\text{RhC}} = 11.0\text{ Hz}$, $J_{\text{PC}} = 1.8\text{ Hz}$); 32.4 (2C, d, cod- CH_2 , $J_{\text{RhC}} = 2.6\text{ Hz}$); 29.1 (2C, d, cod- CH_2 , $J_{\text{RhC}} = 1.6\text{ Hz}$); 26.7 (1C, d, PCH_2 , $^1J_{\text{PC}} = 52.3\text{ Hz}$); 22.8 (1C, dd, PCH_2 , $^1J_{\text{PC}} = 26.6$, $^2J_{\text{RhC}} = 4.1\text{ Hz}$). Anal. Calc. for $\text{C}_{29}\text{H}_{29}\text{F}_6\text{P}_2\text{Pd}_1\text{S}_1\text{Sb}_1$: C, 42.81; H, 3.59. Found: C, 42.99; H, 3.62%.

4.2.3. $[\text{Rh}(\text{cod})((\text{S})\text{-BINAP}(\text{S}))][\text{SbF}_6]$ (**1c**)

^1H NMR (400 MHz, CDCl_3) δ : 8.5 (1H, dd, aromatic-*H*, $J = 8.4\text{ Hz}$, $J = 3.2\text{ Hz}$); 8.18–8.28 (4H, m, aromatic-*H*); 7.89 (3H, m, aromatic-*H*); 7.63–7.77 (7H, m, aromatic-*H*); 7.56 (1H, d, aromatic-*H*, $J = 8.0\text{ Hz}$); 7.35 (4H, m, aromatic-*H*); 7.20 (1H, t, aromatic-*H*, $J = 7.6\text{ Hz}$); 7.14 (1H, t, aromatic-*H*, $J = 7.6\text{ Hz}$); 6.8–7.0 (4H, m, aromatic-*H*); 6.70–6.78 (3H, m, aromatic-*H*); 6.46 (2H, t, aromatic-*H*, $J = 8.8\text{ Hz}$); 6.15 (1H, d, aromatic-*H*, $J = 8.8\text{ Hz}$); 5.06 (1H, m, cod-CH); 4.62 (1H, m, cod-

CH); 3.90 (1H, m, cod-CH); 3.59 (1H, m, cod-CH); 2.34 (1H, m, cod-CH₂); 2.14 (1H, m, cod-CH₂); 1.97 (1H, m, cod-CH₂); 1.60–1.79 (5H, m, cod-CH₂). ³¹P NMR (162 MHz, CDCl₃) δ: 41.14 (P=S); 15.00 (P(III), $J_{Rh-P} = 136$ Hz). ¹³C NMR (126 MHz, CDCl₃) δ: 142.86, 139.11, 125.6–135.6, 112.91, 112.68 (44C, aromatic-C); 98.79 (1C, d, cod-CH, $J_{Rh-C} = 7$ Hz); 93.60 (1C, d, cod-CH, $J_{Rh-C} = 7$ Hz); 82.43 (1C, d, cod-CH, $J_{Rh-C} = 11$ Hz); 81.91 (1C, d, cod-CH, $J_{Rh-C} = 11$ Hz); 32.09 (1C, s, cod-CH₂); 31.86 (1C, s, cod-CH₂); 30.13 (1C, s, cod-CH₂); 29.24 (1C, s, cod-CH₂). No additional fluxional processes were observed upon raising the temperature of the sample in CD₂Cl₂ to 40 °C or in acetone-d₆ to 60 °C.

4.2.4. [Rh(cod)(dppf(S))][SbF₆] (1d)

¹H NMR (500 MHz, CD₂Cl₂, 20 °C) δ: 7.72–7.49 (20H, complex, Ph-H); 4.97 (2H, m, Cp-H); 4.93 (2H, m, Cp-H, $J_{PH} = 1.8$ Hz); 4.81 (2H, m, Cp-H, $J_{PH} = 1.9$ Hz); 4.80 (2H, m, cod-CH); 4.36 (2H, m, Cp-H); 3.79 (2H, m, cod-CH); 2.39 (2H, m, cod-CH₂); 2.24 (2H, m, cod-CH₂); 2.02 (2H, m, cod-CH₂); 1.97 (2H, m, cod-CH₂). ³¹P NMR (202 MHz, CD₂Cl₂) δ: 45.5 (P=S); 19.9 (P(III), d, $J_{RhP} = 147.9$ Hz). ¹³C NMR (101 MHz, CD₂Cl₂) δ: 133.9 (4C, d, Ph-C, $J_{PC} = 11.2$ Hz); 133.5 (2C, d, Ph-C, $J_{PC} = 3.1$ Hz); 132.2 (4C, d, Ph-C, $J_{PC} = 11.1$ Hz); 131.3 (2C, d, Ph-C, $J_{PC} = 1.9$ Hz); 131.0 (2C, d, Ph-CP, $J_{PC} = 43.4$ Hz); 129.4 (2C, d, Ph-CP, $J_{PC} = 87.9$ Hz); 129.2 (4C, d, Ph-C, $J_{PC} = 12.9$ Hz); 128.8 (4C, d, Ph-C, $J_{CP} = 9.9$ Hz); 103.5 (2C, dd, cod-CH, $J_{PC} = 7.2$ Hz, $J_{Rhc} = 11.7$ Hz); 82.5 (2C, d, cod-CH, $J_{Rhc} = 12.9$ Hz); 77.9 (2C, d, Cp-C, $J_{PC} = 8.2$ Hz); 77.2 (2C, d, Cp-C, $J_{PC} = 13.4$ Hz); 74.7 (1C, d, Cp-CP, $J_{PC} = 48.4$ Hz); 74.1 (2C, d, Cp-C, $J_{PC} = 11.1$ Hz); 72.7 (2C, d, Cp-C, $J_{PC} = 5.6$ Hz); 70.1 (1C, d, Cp-CP, $J_{PC} = 95.0$ Hz); 31.9 (2C, m, cod-CH₂); 29.6 (2C, m, cod-CH₂). Anal. Calc. for C₄₂H₄₀F₆FeP₂Rh₁S₁Sb₁: C, 48.82; H, 3.90. Found: C, 48.62; H, 3.82%. No additional fluxional processes were observed on raising the temperature of the sample in CD₂Cl₂ to 40 °C or in acetone-d₆ to 60 °C. Only four backbone Cp protons, as two AA'BB'X multiplets, were observed at room temperature indicating rapid averaging of the enantiomers and conformers of the ferrocenyl moiety. Nevertheless, the observation of distinct cod olefinic protons cis and trans to P showed that *cis-trans* exchange is slow on the NMR time scale at ambient temperature. Lowering the temperature resulted in decoalescence of the cod olefin protons. This would correspond to the averaging of the enantiomers resulting from ligand conformations shown in Scheme 3. At –70 °C the spectrum is complicated by the appearance of diastereomeric conformations of the ferrocenyl moiety in addition to the “up-down” enantiomers shown in Scheme 3. The configuration at the P–Rh–S–P appears to dictate one orientation of the ferrocenyl conformation preferentially and on diastereomeric configuration is preferred over the other in a ratio of 10:1.5. This is most readily observed in the ³¹P NMR which shows two sets of resonances in a ratio of 10:1.5 with ³¹P NMR

(202 MHz, CD₂Cl₂, –20 °C) major δ: 45.5 (P=S); 19.9 (P(III), d, $J_{RhP} = 147.9$ Hz); minor δ: 40.7 (P=S); 22.3 (P(III), d, $J_{RhP} = 149.9$ Hz).

4.2.5. [Rh(cod)(xantphos(S))][SbF₆] (1e)

¹H NMR (500 MHz, CD₂Cl₂, 25 °C) δ: 7.92 (1H, d, aromatic-H, $J_{HH} = 7.9$ Hz); 7.73 (1H, dd, aromatic-H, $J_{HH} = 1.5$ Hz, 7.9 Hz); 7.51 (1H, dt, aromatic-H, $J_{PH} = 1.8$ Hz, $J_{HH} = 7.7$ Hz); 7.37–7.12 (22H, complex, aromatic-H); 6.64 (1H, ddd, aromatic-H, $J_{PH} = 14.8$ Hz, $J_{HH} = 1.4$ Hz, 7.7 Hz); 5.25 (2H, br, cod-CH); 3.33 (2H, br, cod-CH); 1.92 (4H, br, cod-CH₂); 1.79 (6H, s, CH₃); 1.72 (4H, br, cod-CH₂). ³¹P NMR (162 MHz, CD₂Cl₂) δ: 40.5 (P=S); 15.6 (P(III), d, $J_{RhP} = 143.0$ Hz). ¹H NMR (500 MHz, CD₂Cl₂, –70 °C) δ: 8.46 (1H, br, aromatic-H); 7.90–7.67 (7H, v. br, aromatic-H); 7.90 (1H, d, aromatic-H, $J = 8.0$ Hz); 7.72 (1H, d, aromatic-H, $J = 8.0$ Hz); 7.63 (1H, t, aromatic-H, $J = 7.2$ Hz); 7.51 (3H, s, aromatic-H); 7.41 (1H, t, aromatic-H, $J = 7.2$ Hz); 7.26 (3H, t, aromatic-H, $J = 7.2$ Hz); 7.14 (4H, m, aromatic-H); 6.88 (2H, dd, aromatic-H, $J = 7.8$ Hz, 14.7 Hz); 6.59 (1H, dd, aromatic-H, $J = 7.7$ Hz, 14.2 Hz); 6.46 (1H, br, aromatic-H); 5.81 (1H, m, cod-CH); 4.66 (1H, m, cod-CH); 3.75 (1H, m, cod-CH); 2.68 (1H, m, cod-CH₂); 2.24 (3H, m, cod-CH, cod-CH₂); 1.99 (3H, s, CH₃); 1.78 (1H, m, cod-CH₂); 1.57 (1H, m, cod-CH₂); 1.53 (3H, s, CH₃); 1.38 (1H, m, cod-CH₂); 1.02 (1H, m, cod-CH₂); 0.063 (1H, m, cod-CH₂). ¹³C NMR (126 MHz, CD₂Cl₂, –70 °C) δ: 155.9 (1C, m, OC); 153.4 (1C, m, OC); 136.2–125.4, 118.9, 115.0 (34C, aromatic-C); 103.0 (1C, m, cod-CH); 99.1 (1C, m, cod-CH); 90.1 (1C, m, cod-CH); 81.9 (1C, m, cod-CH); 35.9, 33.4, 32.2, 31.4, 30.8, 28.0, 24.6 (7C, cod-CH₂, CH₃, C(CH₃)₂). Anal. Calc. for C₄₇H₄₄F₆O₁P₂Rh₁S₁Sb₁: C, 53.38; H, 4.19. Found: C, 53.26; H, 4.07%. Crystals suitable for X-ray crystallography obtained from a concentrated CH₂Cl₂ solution layered with ether. *Cis-trans* interconversion was observed in CD₂Cl₂ and acetone-d₆ and a lower barrier backbone flip also was observed.

4.3. General procedure for preparation of palladium complexes

4.3.1. [Pd(η³-C₃H₅)(P,P=S)][SbF₆] (2)

[Pd(η³-C₃H₅)Cl]₂ (0.10 mmol) was dissolved in CH₂Cl₂ and an equivalent of the appropriate P,P=S ligand was added to the solution. NaSbF₆ (0.22 mmol) was then added and the mixture was stirred for 6 h at R.T. The solution was filtered through Celite and the solvent removed by rotary evaporation.

4.3.2. [Pd(η³-C₃H₅)(dppm(S))][SbF₆] (2a)

The complex **2a** has previously been prepared with other counter ions [24,41]. The room temperature NMR spectral data are consistent with previous observations on other salts [24,41]. ¹H NMR (500 MHz, CD₂Cl₂, –60 °C) δ: 7.65–7.20 (20H, m, Ph-H); 5.66 (1H, dddd, allyl-H, central, $J_{HH} = 6.0, 6.1, 12.6, 12.6$ Hz); 5.04 (1H, allyl-H, *trans* to

P, *syn*, dd, $^3J_{\text{HH}} = 6.1$ Hz, $J_{\text{PH}} = 6.0$ Hz); 4.34 (1H, allyl-*H*, *cis* to P, *syn*, d, $^3J_{\text{HH}} = 6.1$ Hz); 4.03 (1H, m, CH_2); 3.92 (1H, m, CH_2); 3.66 (1H, allyl-*H*, *trans* to P, *anti*, dd, $^3J_{\text{HH}} = 12.6$ Hz, $J_{\text{PH}} = 10.8$ Hz); 3.09 (1H, allyl-*H*, *cis* to P, *anti*, d, $^3J_{\text{HH}} = 12.6$ Hz). At -20 °C the ^1H resonances at δ 4.34 and δ 3.09 broaden owing to exchange between them and the dppm methylene resonances at δ 4.03 and δ 3.92 also broaden and coalesce. Some averaging of lines within the multiplet at δ 5.66 is also observed at that temperature. Slight broadening of the resonances at δ 5.04 and δ 3.66 only starts to occur upon raising the temperature to 0 °C. ^{31}P NMR (162 MHz, CD_2Cl_2 , 22 °C) δ : 62.3 (P=S, d, $J_{\text{PP}} = 59.6$ Hz); 30.1 (P(III), d, $J_{\text{PP}} = 59.6$ Hz). ^{13}C NMR (101 MHz, CD_2Cl_2 , 20 °C) δ : 134.0 (2C, Ph-C); 133.1 (4C, d, Ph-C, $J_{\text{PC}} = 14.8$ Hz); 133.3 (2C, Ph-C); 132.1 (4C, d, Ph-C, $J_{\text{PC}} = 10.6$ Hz); 129.8 (10C, m, Ph-C); 126.5 (2C, d, Ph-CP, $J_{\text{PC}} = 84.1$ Hz); 120.1 (1C, d, allyl-CH, $J_{\text{PC}} = 5.9$ Hz); 76.2 (1C, br, allyl- CH_2 , *trans* to P, $J_{\text{PC}} \sim 30$ Hz); 65.6 (1C, br, allyl- CH_2 , *cis* to P); 37.9 (1C, dd, PCH_2 , $^1J_{\text{PC}} = 19.9$ Hz, $^1J_{\text{PC}} = 56.7$ Hz).

4.3.3. $[\text{Pd}(\eta^3\text{-C}_3\text{H}_5)(\text{diphos}(S))][\text{SbF}_6]$ (**2b**)

^1H NMR (500 MHz, CD_2Cl_2) δ : 7.90–7.44 (20H, m, Ph-*H*); 5.66 (1H, dddd, allyl-*H*, central, $^3J_{\text{HH}} = 7.0$, 7.6, 12.6, 14.0 Hz); 4.92 (1H, allyl-*H*, *trans* to P, *syn*, ddd, $^4J_{\text{HH}} = 2.0$ Hz, $^3J_{\text{HH}} = 7.6$ Hz, $J_{\text{PH}} = 6.2$ Hz); 3.74 (1H, allyl-*H*, *trans* to P, *anti*, dd, $^3J_{\text{HH}} = 14.0$ Hz, $J_{\text{PH}} = 14.0$ Hz); 3.69 (1H, allyl-*H*, *cis* to P, *syn*, dd, $^4J_{\text{HH}} = 2.0$ Hz, $^3J_{\text{HH}} = 7.0$ Hz); 2.93 (1H, allyl-*H*, *cis* to P, *anti*, d, $^3J_{\text{HH}} = 12.6$ Hz); 3.18–2.80 (4H, m, CH_2). ^{31}P NMR (162 MHz, CD_2Cl_2) δ : 44.1 (P=S, d, $J_{\text{PP}} = 19.8$ Hz); 13.9 (P(III), d, $J_{\text{PP}} = 19.8$ Hz). ^{13}C NMR (126 MHz, CD_2Cl_2) δ : 134.1 (1C, d, Ph-C, $J_{\text{PC}} = 3.0$ Hz); 133.9 (1C, d, Ph-C, $J_{\text{PC}} = 3.0$ Hz); 133.2 (2C, d, Ph-C, $J_{\text{PC}} = 13.0$ Hz); 132.7 (2C, d, Ph-C, $J_{\text{PC}} = 12.6$ Hz); 132.2 (1C, d, Ph-C, $J_{\text{PC}} = 2.5$ Hz); 132.0 (1C, d, Ph-C, $J_{\text{PC}} = 2.5$ Hz); 131.7 (2C, d, Ph-C, $J_{\text{PC}} = 10.4$ Hz); 131.6 (2C, d, Ph-C, $J_{\text{PC}} = 10.4$ Hz); 131.2 (1C, d, Ph-CP, $J_{\text{PC}} = 44.3$ Hz); 130.6 (1C, d, Ph-CP, $J_{\text{PC}} = 44.8$ Hz); 130.1 (2C, d, Ph-C, $J_{\text{PC}} = 12.2$ Hz); 130.0 (2C, d, Ph-C, $J_{\text{PC}} = 12.2$ Hz); 129.9 (2C, d, Ph-C, $J_{\text{PC}} = 10.2$ Hz); 129.8 (2C, d, Ph-C, $J_{\text{PC}} = 10.2$ Hz); 128.0 (1C, d, Ph-CP, $J_{\text{CP}} = 82.5$ Hz); 127.8 (1C, d, Ph-CP, $J_{\text{PC}} = 84.1$ Hz); 120.3 (1C, d, allyl-CH, $J_{\text{PC}} = 6.0$ Hz); 80.3 (1C, dd, allyl- CH_2 , *trans* to P, $J_{\text{PC}} = 28.3$ Hz, 1.6 Hz); 66.2 (1C, d, allyl- CH_2 , *cis* to P, $J_{\text{PC}} = 3.2$ Hz); 26.2 (1C, d, PCH_2 , $^1J_{\text{PC}} = 52.9$ Hz); 22.1 (1C, dd, PCH_2 , $^1J_{\text{PC}} = 26.5$, $^2J_{\text{PC}} = 5.1$ Hz). Anal. Calc. for $\text{C}_{29}\text{H}_{29}\text{F}_6\text{P}_2\text{PdSSb}$: C, 42.81; H, 3.59. Found: C, 42.99; H, 3.62%.

4.3.4. $[\text{Pd}(\eta^3\text{-C}_3\text{H}_5)(\text{dppf}(S))][\text{SbF}_6]$ (**2d**)

^1H NMR (500 MHz, CD_2Cl_2) δ : 7.75–7.67 (6H, m, Ph-*H*); 7.60–7.43 (12H, m, Ph-*H*); 7.40–7.35 (2H, m, Ph-*H*); 5.58 (1H, dddd, allyl-*H*, central, $^3J_{\text{HH}} = 6.9$ Hz, 7.5 Hz, 12.8 Hz, 14.2 Hz); 4.76 (1H, m, Cp-*H*); 4.71 (3H, m, Cp-*H*); 4.54 (3H, m, Cp-*H*); 4.45 (1H, m, Cp-*H*); 4.12 (1H,

ddd, allyl-*H*, *trans* to P, *syn*, $^4J_{\text{HH}} = 2.5$ Hz, $^3J_{\text{HH}} = 7.5$ Hz, $J_{\text{PH}} = 7.2$ Hz); 3.71 (1H, ddd, allyl-*H*, *cis* to P, *syn*, $^4J_{\text{HH}} = 2.2$ Hz, $^3J_{\text{HH}} = 6.9$ Hz, $J_{\text{PH}} = 2.2$ Hz); 3.12 (1H, dd, allyl-*H*, *trans* to P, *anti*, $^3J_{\text{HH}} = 14.2$ Hz, $J_{\text{PH}} = 10.6$ Hz); 3.17 (1H, d, allyl-*H*, *cis* to P, *anti*, $^3J_{\text{HH}} = 12.8$ Hz). ^{31}P NMR (162 MHz, CD_2Cl_2) δ : 42.2 (P=S); 19.3 (P(III)). ^{31}P NMR (162 MHz, CD_2Cl_2) δ : 46.7 (P=S); 18.1 (P(III)). Anal. Calc. for $\text{C}_{37}\text{H}_{33}\text{F}_6\text{Fe}_1\text{P}_2\text{-Pd}_1\text{S}_1\text{Sb}_1$: C, 45.83; H, 3.43. Found: C, 45.70; H, 3.42%. At -100 °C, the complex exists as two diastereomers in a 1.0:0.6 ratio that involve exchange by a twist of the ligand backbone which has a barrier of 10.6 kcal mol $^{-1}$. ^{31}P NMR (162 MHz, CD_2Cl_2 , -100 °C) Major diastereomer δ : 46.9 (P=S); 16.7 (P(III)). Minor diastereomer δ : 46.8 (P=S); 18.0 (P(III)).

4.3.5. $[\text{Pd}(\eta^3\text{-C}_3\text{H}_5)(\text{xantphos}(S))][\text{SbF}_6]$ (**2e**)

^1H NMR (400 MHz, CD_2Cl_2) δ : 7.85 (1H, ddd, xanthene-*H*, $^4J_{\text{HH}} = 1.4$ Hz, $^3J_{\text{HH}} = 7.9$ Hz, $^5J_{\text{PH}} = 1.0$ Hz); 7.72 (1H, dd, xanthene-*H*, $^4J_{\text{HH}} = 1.4$ Hz, $^3J_{\text{HH}} = 7.9$ Hz); 7.66–7.18, 7.07 (22H, m, Ph-*H*, xanthene-*H*); 6.76 (1H, ddd, xanthene-*H*, $^4J_{\text{HH}} = 1.4$ Hz, $^3J_{\text{HH}} = 7.9$ Hz, $^3J_{\text{PH}} = 10.2$ Hz); 6.65 (1H, ddd, xanthene-*H*, $^4J_{\text{HH}} = 1.4$ Hz, $^3J_{\text{HH}} = 7.9$ Hz, $^3J_{\text{PH}} = 15.2$ Hz); 5.29 (1H, dddd, allyl-*H*, central, $^3J_{\text{HH}} = 6.9$ Hz, 7.5 Hz, 12.8 Hz, 13.6 Hz); 4.72 (1H, allyl-*H*, *trans* to P, *syn*, ddd, $^4J_{\text{HH}} = 2.2$ Hz, $^3J_{\text{HH}} = 7.5$ Hz, $J_{\text{PH}} = 7.3$ Hz); 3.72 (1H, allyl-*H*, *cis* to P, *syn*, dd, $^4J_{\text{HH}} = 2.2$ Hz, $^3J_{\text{HH}} = 6.8$ Hz); 3.25 (1H, allyl-*H*, *trans* to P, *anti*, dd, $^3J_{\text{HH}} = 13.6$ Hz, $J_{\text{PH}} = 10.6$ Hz); 2.30 (1H, allyl-*H*, *cis* to P, *anti*, d, $^3J_{\text{HH}} = 12.8$ Hz); 1.79 (3H, s, CH_3); 1.67 (3H, s, CH_3). ^{31}P NMR (162 MHz, CD_2Cl_2) δ : 42.2 (P=S); 19.3 (P(III)). ^{13}C NMR (126 MHz, CD_2Cl_2) δ : 155.0 (1C, m, OC); 153.2 (1C, m, OC); 134.6–128.9, 125.8, 125.1, 119.3, 119.0, 116.2, 115.5 (34C, aromatic-C); 119.4 (1C, d, allyl-CH, $J_{\text{PC}} = 6.0$ Hz); 80.1 (1C, d, allyl- CH_2 , *trans* to P, $J_{\text{PC}} = 32.3$ Hz); 66.2 (1C, d, allyl- CH_2 , *cis* to P, $J_{\text{PC}} = 2.2$ Hz) 35.4, 30.8, 28.2 (3C, $\text{C}(\text{CH}_3)_2$, CH_3). Anal. Calc. for $\text{C}_{42}\text{H}_{37}\text{F}_6\text{OP}_2\text{PdSSb}$: C, 50.75; H, 3.75. Found: C, 50.65; H, 3.70%.

4.3.6. Preparation of $\text{Pd}(\text{HC}(\text{PPh}_2)(\text{P}(S)\text{Ph}_2)_2)\text{Cl}_2$ (**3**)

The *bis*-sulfide of 1,1,1-tris-diphenylphosphinomethane · LiCl (0.26 mmol, 17.6 mg) was combined with Pd($\text{C}_6\text{H}_5\text{CN}$) $_2\text{Cl}_2$ in dry CH_2Cl_2 and stirred at R.T. for 30 min, then filtered through Celite. The solvent was removed by rotary evaporation and the resulting orange solid was washed with ether and the desired product was collected in 78% yield. ^{31}P NMR (162 MHz, CD_2Cl_2 , -80 °C) δ : 64.1 (P=S, d, $^2J_{\text{PP}} = 47$ Hz); 52.1 (P(III), dd, $^2J_{\text{PP}} = 47$, 5 Hz); 33.6 (P=S, d, $^2J_{\text{PP}} = 5$ Hz). Anal. Calc. for $\text{C}_{37}\text{H}_{31}\text{Cl}_2\text{P}_3\text{Pd}_1\text{S}_2 \cdot 0.25$ CH_2Cl_2 : C, 53.82; H, 3.82. Found: C, 53.48; H, 3.80%.

4.3.7. Preparation of $[\text{Pd}(\eta^3\text{-C}_3\text{H}_5)(\text{HC}(\text{PPh}_2)(\text{P}(S)\text{Ph}_2)_2)][\text{SbF}_6]$ (**4**)

$[\text{Pd}(\eta^3\text{-C}_3\text{H}_5)\text{Cl}]_2$ (125 mg, 0.34 mmol) was dissolved in CH_2Cl_2 (10 mL) in a Schlenk flask. To the yellow solution

was added NaSbF₆ (177 mg, 0.68 mmol) and HC(PPh₂)-(P(S)Ph₂)₂·LiCl (461 mg, 0.68 mmol). The mixture was stirred for 6 h, and filtered through Celite. The product was obtained in 83% yield after being crystallized from a concentrated CH₂Cl₂ solution by vapor diffusion of ether. ¹H NMR (500 MHz, CD₂Cl₂, -60 °C) δ: 8.10 (1H, m, Ph-H); 7.82 (2H, m, Ph-H); 7.49 (2H, m, Ph-H); 7.37 (3H, m, Ph-H); 7.28–6.96 (20H, m, Ph-H); 6.89 (2H, m, Ph-H); 5.70 (1H, m, PCH); 5.69 (1H, apparent tt, allyl-H, central, ³J_{HH} ~7.1, 13.1 Hz); 5.06 (1H, apparent t, allyl-H, trans to P, syn, J ~7.1 Hz); 3.80 (1H, br d, allyl-H, cis to P, syn, J ~7.1 Hz); 3.73 (1H, dd, allyl-H, trans to P, anti, ³J_{HH} = 13.2 Hz, J_{PH} = 11.0 Hz); 2.87 (1H, d, allyl-H, cis to P, anti, ³J_{HH} = 12.9 Hz); ³¹P NMR (202 MHz, CD₂Cl₂, -60 °C) δ: 53.9 (P=S, br); 47.2 (P=S, br); 46.4 (P(III), dd, ²J_{PP} = 30.2, 46.0 Hz). Anal. Calc. for C₃₉H₃₃F₆O₁P₂Pd₁S₁Sb₁·0.5 CH₂Cl₂: C, 45.96; H, 3.52. Found: C, 46.03; H, 3.59%.

4.3.8. Preparation of [Pd(C(PPh₂)(P(S)Ph₂)₂)(allyl)] (5)

Complex **4** (50 mg, 0.049 mmol) was dissolved in dry thf and treated with excess NEt₃ (0.014 mL, 0.01 mmol). The solvent was removed by rotary evaporation and the resulting orange solid was immediately dissolved in CDCl₃. Attempts to recrystallize pure material were unsuccessful owing to decomposition. ¹H NMR showed the absence of a resonance at δ 5.70 showing the ligand backbone was deprotonated. ¹H NMR (400 MHz, CDCl₃, 22 °C) δ: 8.18–6.90 (30H, m, Ph-H); 5.23 (1H, apparent tt, allyl-H, central, ³J_{HH} ~7.0, 13.0 Hz); 4.40 (1H, apparent t, allyl-H, trans to P, syn, J ~6.4 Hz); 3.32 (1H, br d, allyl-H, cis to P, syn, J ~7.4 Hz); 3.11 (1H, dd, allyl-H, trans to P, anti, ³J_{HH} = 13.5 Hz, J_{PH} = 10.0 Hz); 2.45 (1H, d, allyl-H, cis to P, anti, ³J_{HH} = 12.5 Hz). ³¹P NMR (162 MHz, CDCl₃, 22 °C) δ: 62.3 (dd, ²J_{PP} = 48.0, 120.5 Hz); 43.8 (dd, ²J_{PP} = 48.0, 19.8 Hz); 34.3 (dd, ²J_{PP} = 19.8, 120.5 Hz).

4.4. Synthesis of P,P=S ligands

Only Xantphos(S) has not been previously reported (see Section 4.1 for references).

4.4.1. Xantphos(S) (e)

Yield: 88%. ¹H NMR (500 MHz, CD₂Cl₂) δ: 7.81 (4H, m, Ph-H); 7.68 (1H, ddd, xanthene-H, ⁴J_{HH} = 1.4 Hz, ³J_{HH} = 7.9 Hz, J_{PH} = 1.0 Hz); 7.43 (1H, dd, xanthene-H, ⁴J_{HH} = 1.4 Hz, ³J_{HH} = 7.9 Hz); 7.38–7.34 (3H, m, Ph-H); 7.29–7.21 (10H, Ph-H, xanthene-H); 7.12 (1H, dt, xanthene-H, ⁴J_{PH} = 2.0 Hz, ³J_{HH} = 7.9 Hz); 6.94 (5H, m, Ph-H); 6.59 (1H, ddd, xanthene-H, ⁴J_{HH} = 1.4 Hz, ³J_{HH} = 7.9 Hz, J_{PH} = 3.2 Hz); 1.65 (6H, s, CH₃). ³¹P NMR (202 MHz, CD₂Cl₂) δ: 41.1 (P=S); -22.6 (P(III)). ¹³C NMR (126 MHz, CD₂Cl₂) δ: 152.8 (1C, m, OC); 152.1 (1C, m, OC); 139.1–119.8 (34 C, aromatic-C) 32.8 (2C, C(CH₃)₂). Anal. Calc. for C₃₉H₄₂OP₂S: C, 76.70; H, 5.28. Found: C, 76.31; H, 5.44%.

4.4.2. HC(PPh₂)(P(S)Ph₂)₂

This compound was prepared previously [37]. The bis-sulfide was prepared by adding a 1.8 mole ratio of sulfur to a solution of 1,1,1-tris-diphenylphosphinomethane (P:S, 3:1.8) in CH₂Cl₂ in a Schlenk flask and stirred at R.T. After 16 h, ³¹P NMR showed the product was a mixture of the *mono* and *bis*-sulfides by comparison to literature data. These were separated by column chromatography (silica gel, 3:1 CH₂Cl₂:hexane) giving 49% yield of the *bis*-sulfide. An unusual feature of this compound is that the *bis*-sulfide elutes first and the *mono*-sulfide second. It is generally observed when using *bis*-phosphines for the analogous reaction that the unreacted *bis*-phosphine elutes first, the *mono*-sulfide second, and the *bis*-sulfide last.

4.5. Structure determination and refinement

Data were collected on a Nonius KappaCCD (Mo Kα radiation) diffractometer at -100 °C and were not specifically corrected for absorption other than the inherent corrections provided by Scalepack [46]. The structures were solved by direct methods (SIR-92) [47] and refined on *F* for all reflections [48]. Nonhydrogen atoms were refined with anisotropic displacement parameters. Hydrogen atoms were included at calculated positions. Relevant crystal and data parameters are presented in Table 3. Atomic coordinates were deposited with the Cambridge Crystallographic Data Centre.

4.5.1. [Rh(cod)(Ph₂PCH₂P(S)Ph₂)]/[SbF₆] (1a)

Crystals were obtained by slow diffusion of pentane into a chloroform solution of **1a**. This complex crystallized with one molecule of chloroform in the asymmetric unit in the hexagonal space group *P*6₁ and the correct chirality and space group determined by inverting the coordinates. The inverted structure gave an *R* and *wR* of 0.0309 and 0.0355 vs. 0.00302 and 0.0350 for the correct hand. Angles of 89.32(6)° for P–Rh–S. and 107.01(9)° for Rh–S–P and bond distances of Rh–S of 2.344(2) Å and Rh–P of 2.264(2) Å were found.

4.5.2. [Rh(cod)(xantphos(S))]/[SbF₆] (1e)

Orange crystals were obtained by slow diffusion of diethyl ether into a methylene chloride solution of **1e**. This complex crystallized in the triclinic space group *P* $\bar{1}$. Angles of 92.99(4)° for P–Rh–S and 108.47(5)° for Rh–S–P and bond distances of Rh–S of 2.400(1) Å and Rh–P of 2.331(2) Å were found.

4.5.3. [Pd(η³-C₃H₅)(xantphos(S))]/[SbF₆] (2e)

Pale yellow crystals were obtained by slow diffusion of diethyl ether into a methylene chloride solution of **2e**. This complex crystallized in the triclinic space group *P* $\bar{1}$ with two cations, two anions, and one molecule of diethyl ether in the asymmetric unit. The two independent cations only showed minor differences in metrical parameters. Both

Table 3
Crystallographic data for **1a**, **1e**, and **4**

	1a	1e	4
Color, shape	Yellow block	Orange block	Pale yellow needle
Empirical formula	C ₃₄ H ₃₅ Cl ₃ F ₆ P ₂ RhSSb	C ₄₇ H ₄₄ F ₆ OP ₂ RhSSb	C ₄₂ H ₄₁ F ₆ O _{0.5} P ₃ PdS ₂ Sb
Formula weight	982.66	1057.52	1052.97
Radiation (Å)	Mo Kα (monochr.) 0.71073	Mo Kα (monochr.) 0.71073	Mo Kα (monochr.) 0.71073
T (K)	173	173	173
Crystal system	Hexagonal	Triclinic	Triclinic
Space group	P6 ₁ (No. 169)	P $\bar{1}$ (No. 2)	P $\bar{1}$ (No. 2)
<i>Unit cell dimensions</i>			
a (Å)	11.7862 (3)	11.7147(3)	11.1929(2)
b (Å)		11.8044(3)	11.2082(2)
c (Å)	46.949(1)	15.8139(3)	33.3241(6)
α (°)		85.380(2)	91.9370(11)
β (°)		78.843(2)	91.3291(11)
γ (°)		85.967(2)	90.0841(9)
V (Å ³)	5648.1(2)	2135.17(9)	4177.06(11)
Z	6	2	4
D _{calc} (g cm ⁻³)	1.733	1.645	1.674
μ (cm ⁻¹) (Mo Kα)	15.61	12.04	13.50
Crystal size (mm)	0.07 × 0.12 × 0.12	0.10 × 0.12 × 0.12	0.10 × 0.12 × 0.22
Total reflections, unique reflections	8490, 6183	16685, 9740	31820, 18762
R _{int}	0.032	0.029	0.037
Number of observation (I > 3σ(I))	3410	6065	11083
Parameters, constraints	432, 0	532, 0	1018, 0
R ^a , wR ^b , GOF	0.030, 0.035, 1.09	0.035, 0.035, 1.33	0.040, 0.043, 1.58
Residual density (e Å ⁻³)	-0.52 < 0.42	-0.67 < 0.72	-0.68 < 0.83

^a $R = \sum ||F_o| - |F_c|| / \sum |F_o|$, for all $I > 3\sigma(I)$.

^b $wR = [\sum [w(|F_o| - |F_c|)^2] / \sum [w(F_o)^2]]^{1/2}$.

cations showed a 2:1 disorder in the orientation of the allyl as indicated by common positions for the terminal carbons of the allyl and the central carbon distributed above and below the S–Pd–P plane. Angles of 94.78(5)° for P–Pd–S, and 98.93(7) for Pd–S–P and bond distances of Pd–S of 2.336(2) Å, Pd–P of 2.280(2) Å, Pd–C1 (*trans* to P) of 2.191(6) Å, Pd–C3 (*trans* to S) of 2.132(6) Å were found for one cation. Analogous angles of 94.72(5)° for P–Pd–S, and 99.75(7) for Pd–S–P and bond distances of Pd–S of 2.332(2) Å, Pd–P of 2.276(2) Å, Pd–C1' (*trans* to P) of 2.174(5) Å, Pd–C3' (*trans* to S) of 2.122(5) Å were found for the other cation.

Acknowledgements

We thank the donors of the Petroleum Research Fund administered by the American Chemical Society for support of our work (PRF#43212).

Appendix A. Supplementary material

CCDC 656278, 656277 and 656276 contain the supplementary crystallographic data for **1a**, **1e** and **4**. These data can be obtained free of charge from The Cambridge Crystallographic Data Centre via www.ccdc.cam.ac.uk/data_request/cif, or from the Cambridge Crystallographic Data Centre, 12 Union Road, Cambridge CB2 1EZ, UK; fax: (+44) 1223-336-033; or e-mail: deposit@ccdc.cam.ac.uk. Supplementary data associated with this article

can be found, in the online version, at [doi:10.1016/j.jorganchem.2007.10.044](https://doi.org/10.1016/j.jorganchem.2007.10.044).

References

- [1] F.A. Cotton, J. Organometal. Chem. 100 (1975) 29.
- [2] A. Bader, E. Lindner, Coord. Chem. Rev. 108 (1991) 27.
- [3] P. Braunstein, F. Naud, Angew. Chem., Int. Ed. 40 (2001) 680.
- [4] P. Braunstein, J. Organometal. Chem. 689 (2004) 3953.
- [5] C.S. Slone, D.A. Weinberger, C.A. Mirkin, Prog. Inorg. Chem. 48 (1999) 233.
- [6] W. Keim, Angew. Chem., Int. Ed. Engl. 29 (1990) 235.
- [7] G.J.P. Britovsek, W. Keim, S. Mecking, D. Sainz, T. Wagner, J. Chem. Soc., Chem. Commun. (1993) 1632.
- [8] E. Drent, R. van Dijk, R. van Ginkel, B. van Oort, R.I. Pugh, Chem. Commun. (2002) 744.
- [9] E. Drent, J.A.M. vanBroekhoven, P.H.M. Budzelaar, Rec. Trav. Chim. Pays Bas 115 (1996) 263.
- [10] M.J. Szabo, N.M. Galea, A. Michalak, S.Y. Yang, L.F. Groux, W.E. Piers, T. Ziegler, J. Am. Chem. Soc. 127 (2005) 14692.
- [11] J.W. Faller, B.J. Grimmond, D.G. D'Allesi, J. Am. Chem. Soc. 123 (2001) 2525.
- [12] G. Helmchen, A. Pfaltz, Acc. Chem. Res. 33 (2000) 336.
- [13] D.A. Evans, K.R. Campos, J.S. Tedrow, F.E. Michael, M.R. Gagne, J. Am. Chem. Soc. 122 (2000) 7905.
- [14] J. Sprinz, M. Kiefer, G. Helmchen, G. Huttner, O. Walter, L. Zsolnai, M. Reggelin, Tetrahedron Lett. 35 (1994) 1523.
- [15] J.W. Faller, J.C. Wilt, J. Parr, Org. Lett. 6 (2004) 1301.
- [16] J.W. Faller, J.C. Wilt, Organometallics 24 (2005) 5076.
- [17] J.W. Faller, N.J. Zhang, K.J. Chase, W.K. Musker, A.R. Amaro, C.M. Semko, J. Organometal. Chem. 468 (1994) 175.
- [18] S. Komiya, T.A. Albright, R. Hoffmann, J.K. Kochi, J. Am. Chem. Soc. 98 (1976) 7255.
- [19] D.L. Thorn, R. Hoffmann, J. Am. Chem. Soc. 100 (1978) 2079.

- [20] K. Tatsumi, R. Hoffmann, A. Yamamoto, J.K. Stille, *Bull. Chem. Soc. Jpn.* 54 (1981) 1857.
- [21] T.J. McCarthy, R.G. Nuzzo, G.M. Whitesides, *J. Am. Chem. Soc.* 103 (1981) 1676.
- [22] R.J. van Haaren, K. Goubitz, J. Fraanje, G.P.F. van Strijdonck, H. Oevering, B. Coussens, J.N.H. Reek, P.C.J. Kamer, P. van Leeuwen, *Inorg. Chem.* 40 (2001) 3363.
- [23] J.W. Faller, J.C. Wilt, *J. Organometal. Chem.* 691 (2006) 2207.
- [24] H. Valentini, K. Selvakumar, M. Worle, P.S. Pregosin, *J. Organometal. Chem.* 587 (1999) 244.
- [25] J. Herrmann, P.S. Pregosin, R. Salzmänn, A. Albinati, *Organometallics* 14 (1995) 3311.
- [26] J.W. Faller, M.E. Thomsen, M.J. Mattina, *J. Am. Chem. Soc.* 93 (1971) 2642.
- [27] P. Dierkes, P. van Leeuwen, *J. Chem. Soc., Dalton Trans.* (1999) 1519.
- [28] O. Piechaczyk, M. Doux, L. Ricard, P. le Floch, *Organometallics* 24 (2005) 1204.
- [29] T.Y.H. Wong, S.J. Rettig, B.R. James, *Inorg. Chem.* 38 (1999) 2143.
- [30] J.W. Faller, P.P. Fontaine, *J. Organometal. Chem.* 692 (2007) 976.
- [31] J.W. Faller, J.C. Wilt, *Org. Lett.* 7 (2005) 633.
- [32] R. Broussier, E. Bentabet, M. Laly, P. Richard, L.G. Kuz'mina, P. Serp, N. Wheatley, P. Kalck, B. Gautheron, *J. Organometal. Chem.* 613 (2000) 77.
- [33] A. Rufinska, R. Goddard, C. Weidenthaler, M. Buhl, K.R. Porschke, *Organometallics* 25 (2006) 2308.
- [34] J.W. Faller, M.J. Incorvia, *J. Organometal. Chem.* 19 (1969) P13.
- [35] A. Gogoll, J. Ornebro, H. Grennberg, J.E. Backvall, *J. Am. Chem. Soc.* 116 (1994) 3631.
- [36] S. Hansson, P.O. Norrby, M.P.T. Sjogren, B. Akermark, M.E. Cucciolito, F. Giordano, A. Vitagliano, *Organometallics* 12 (1993) 4940.
- [37] P. Barbaro, P.S. Pregosin, R. Salzmänn, A. Albinati, R.W. Kunz, *Organometallics* 14 (1995) 5160.
- [38] B.M. Trost, M.H. Hung, *J. Am. Chem. Soc.* 106 (1984) 6837.
- [39] G. Giordano, R.H. Crabtree, *Inorg. Synth.* 19 (1979) 218.
- [40] T. Hayashi, A. Yamamoto, Y. Ito, E. Nishioka, H. Miura, K. Yanagi, *J. Am. Chem. Soc.* 111 (1989) 6301.
- [41] J. Browning, K.R. Dixon, S.F. Wang, *J. Organometal. Chem.* 474 (1994) 199.
- [42] S.O. Grim, E.D. Walton, *Inorg. Chem.* 19 (1980) 1982.
- [43] E.I. Matrosov, Z.A. Starikova, A.I. Yanovsky, D.I. Lobanov, I.M. Aladzheva, O.V. Bykhovskaya, Y.T. Struchkov, T.A. Mastryukova, M.I. Kabachnik, *J. Organometal. Chem.* 535 (1997) 121.
- [44] G. Pilloni, B. Longato, G. Bandoli, *Inorg. Chim. Acta* 277 (1998) 163.
- [45] T.C. Blagborough, R. Davis, P. Ivison, *J. Organometal. Chem.* 467 (1994) 85.
- [46] W. Minor, Z. Otwinowski (Eds.), *HKL2000 (Denzo-SMN) software package. Processing of X-ray Diffraction Data Collected in Oscillation Mode, Methods in Enzymology, Macromolecular Crystallography*, Academic Press, New York, 1997.
- [47] A. Altomare, G. Casciarano, C. Giacovazzo, A. Guagliardi, *J. Appl. Crystallogr.* 26 (1993) 343.
- [48] Texsan, *TEXSAN for Windows version 1.06: Crystal Structure Analysis Package*, Molecular Structure Corporation (1997–1999), 1999.